ERDC/CHL TR-13-9

US Army Corps
of Engineers®
Engineer Research and
Development Center

ERDC
INNOVATIVE SOLUTIONS
for a safer, better world

Navigation Systems Research Program

Validation of Modeling Flow Approaching Navigation Locks

Carlos B. Bislip-Morales and Richard L. Stockstill

August 2013

Coastal and Hydraulics Laboratory

The US Army Engineer Research and Development Center (ERDC) solves the nation's toughest engineering and environmental challenges. ERDC develops innovative solutions in civil and military engineering, geospatial sciences, water resources, and environmental sciences for the Army, the Department of Defense, civilian agencies, and our nation's public good. Find out more at www.erdc.usace.army.mil.

To search for other technical reports published by ERDC, visit the ERDC online library at http://acwc.sdp.sirsi.net/client/default.

Navigation Systems Research Program

ERDC/CHL TR-13-9
August 2013

Validation of Modeling Flow Approaching Navigation Locks

Carlos B. Bislip-Morales and Richard L. Stockstill

Coastal and Hydraulics Laboratory
US Army Engineer Research and Development Center
3909 Halls Ferry Road
Vicksburg, MS 39180-6199

Final report

Prepared for US Army Corps of Engineers
441 G. Street, NW
Washington, DC 20314-1000

Abstract

Experiments were conducted to assess the ability of the 2D depth-averaged numerical flow solver AdH to compute flow conditions in the approach to navigation locks. The velocity distribution computed with the numerical model was compared with similar data obtained on a physical model. The simulation results of two bathymetric configurations were evaluated. The Plan A lock approach had a rather simple bed geometry with a fairly flat bottom and simple side slopes. The Plan B lock approach had a series of submerged weirs upstream of the guard wall, placed normal to the navigation sailing line. Other than the flow between the guard wall cells, the numerical model accurately reproduced the flow distribution, velocity magnitudes, and directions compared in the Plan A lock approach; however, the numerical model did not accurately reproduce the velocity with the Plan B lock approach. Experiments were conducted to determine if reasonable changes to model parameters could result in more accurate numerical model results. Extending the weir material had an effect; however, it was not sufficient to reproduce the observed data. The accuracy of the velocity of the flow between the guard wall cells did not improve in either case. These effects are attributed to both the mild-slope and hydrostatic pressure assumptions.

Contents

Figures

Figures

Preface

The investigation reported herein was sponsored by the Navigation Systems Research Program (NSRP). This work was conducted in the Coastal and Hydraulics Laboratory (CHL) of the US Army Engineer Research and Development Center (ERDC). The model validation was conducted during the period of July 2011 to November 2011 as part of the NSRP work unit "Modeling Lock Approaches."

This research was conducted under the general direction of Dr. William D. Martin, Director of the CHL; Jose E. Sanchez, Deputy Director, CHL; Dr. Rose Kress, Chief of the Navigation Division, CHL; and Dr. Richard B. Styles, Chief of the Navigation Branch (HN), CHL. Navigation branch personnel conducted both physical and numerical models of the Montgomery project. In particular, Dr. Stephen T. Maynord, HN, provided technical guidance on the physical model data acquisition portion of the study. Howard E. Park and Cecil C. Dorrel, HN, led the original navigation model study and David Maggio and Keith K. Green, HN, were responsible for the validation experiments. E. Allen Hammack, HN, conducted a numerical model study that served as a design aid to the navigation model study.

The validation study and subsequent report was completed by Carlos B. Bislip-Morales and Dr. Richard L. Stockstill, HN. Acknowledgments are made to Charles E. Wiggins, Navigation Systems Research Program Manager, and Jeff Lillycrop, Technical Director for Navigation, ERDC.

At the time of this report, COL Kevin J. Wilson was Commander and Executive Director of ERDC. Dr. Jeffery P. Holland was Director.

Unit Conversion Factors

Multiply	By	To Obtain
cubic feet	0.02831685	cubic meters
feet	0.3048	meters
miles (US statute)	1,609.347	meters
square feet	0.09290304	square meters

1 Introduction

Background

Montgomery Locks and Dam is located in Monaca, Pennsylvania, on the Ohio River at mile marker 31.7 (Figure 1). Monaca is about 25 miles northwest of Pittsburgh. Constructed from 1932 to 1936, Montgomery Locks and Dam has a gated dam to permit increased control over the water level in the navigation pool upriver of the dam. The project is comprised of a 1,379-ft gated dam, a 110-ft by 600-ft main lock, and a 56-ft by 360-ft auxiliary lock which provide for a 17.5-ft vertical lift.

Figure 1. Vicinity map.

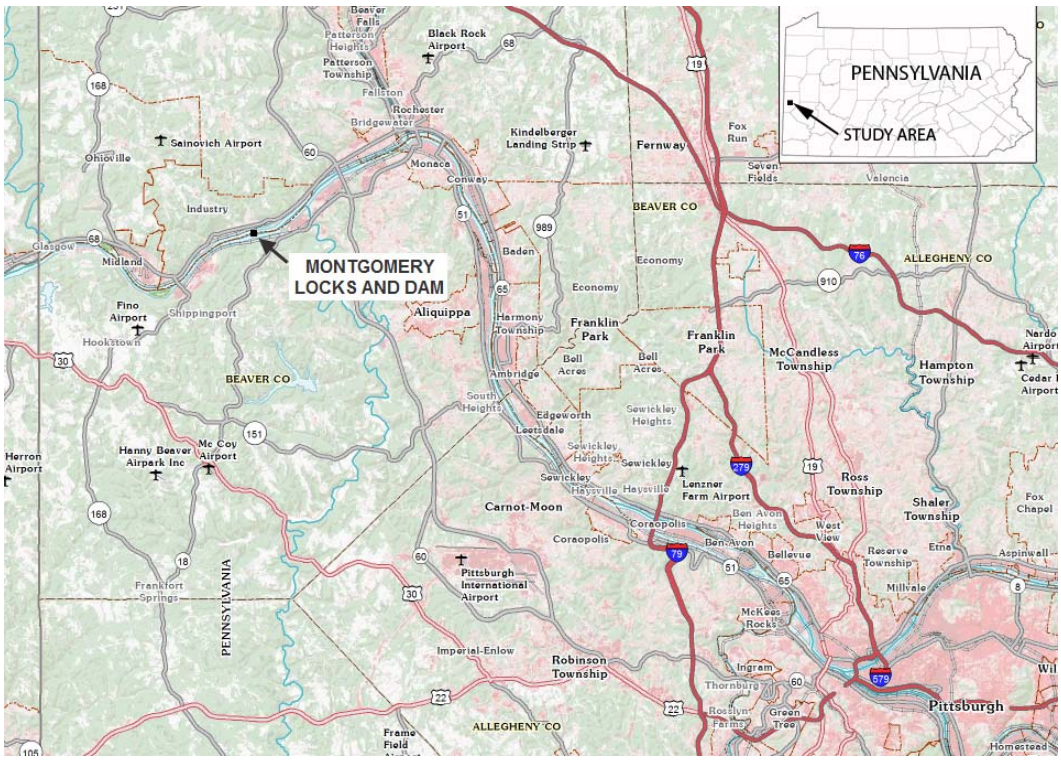

A formal investigation following the 2005 sinking of the M/V Elizabeth M and six barges with four fatalities recommended that the US Army Corps of Engineers (USACE) develop a single definition and a process of determining when the upper Ohio River is in a state of *high water* and methodologies to reduce hazards associated with operations during this state. As a response, the USACE, Pittsburgh District (LRP) requested that the US Army Engineer Research and Development Center, Coastal and

Hydraulics Laboratory (CHL), evaluate the navigation conditions in the Ohio River upstream of Montgomery Locks and Dam. A physical model study of the upper approach was conducted to evaluate the navigation conditions and to make recommendations for channel improvement.

A fixed bed physical model was built to study potential improvements to an existing outdraft problem at Montgomery Locks and Dam. The undistorted 1:100-scale physical model covered approximately 1900 square feet and reproduced about 1.7 miles of the existing river channel and adjacent overbank upstream of the upper guard wall to about river mile 29.6, equivalent to about 9,000 ft of the prototype's upstream approach. Figure 2 illustrates the model limits. Physical models built to 1:100-scale are commonly used to evaluate navigation conditions for tows entering and leaving lock approaches, bridge reach studies, and floodgate studies.

Figure 2. Navigation chart with physical model limits.

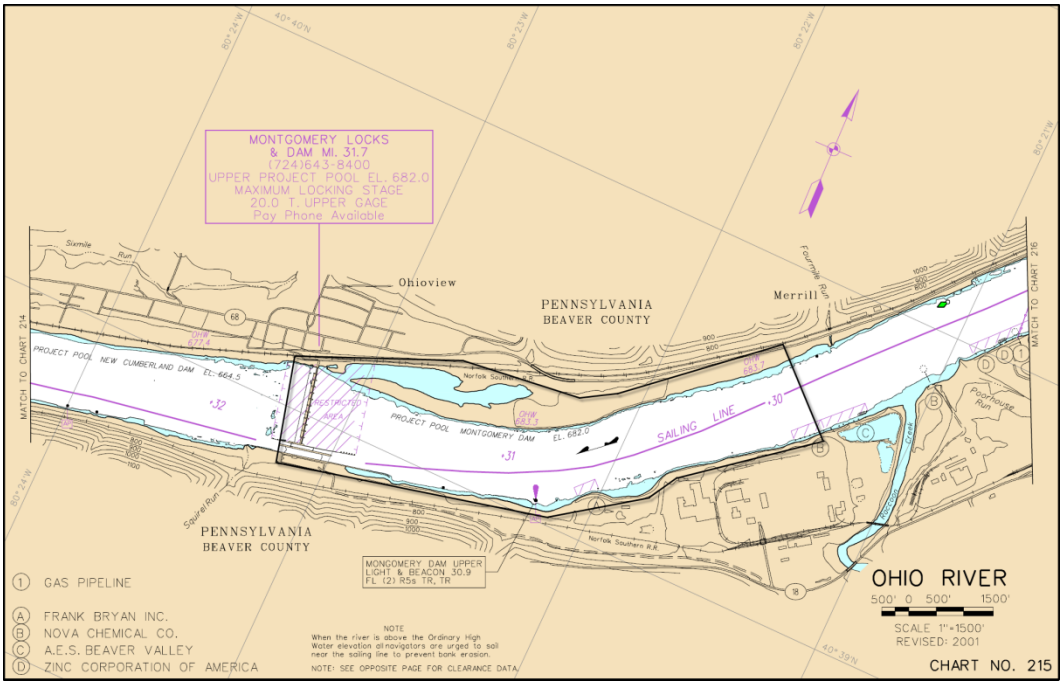

Once the navigation conditions study was completed, the physical model was available for conducting generalized experiments, which provided a means of validating a computational flow model. This report describes the validation of a depth-averaged two-dimensional (2D) flow solver with the intent of using numerical methods to compute flow conditions in lock approaches. Numerical models could be used to supplement physical models for navigation studies. If navigation conditions could be studied

with numerical models, the cost of these studies would be reduced, and it would be feasible to evaluate the approaches to several navigation projects that have recently been identified as having navigation safety issues.

This validation study evaluated two upper approach configurations. Experiments were conducted with and without weirs in the lock approach. The first configuration, referred to as Plan A lock approach, was a river channel approaching the lock and dam. The second set of experiments considered a design, referred to as Plan B lock approach, which contained the weir field in the lock approach. The weirs were used to reduce velocities in the lock approach by training the flow toward the thalweg.

Purpose

The purpose of the study was to assess the ability of a 2D depth-averaged numerical flow model to simulate flow conditions in lock approaches. The Montgomery Locks and Dam physical model provided an opportunity to validate the 2D numerical modeling method. Velocity data were obtained on the physical model for direct comparison with computed results. This model assessment determined the capabilities and limitations of the 2D numerical modeling method.

Approach

Current magnitudes and directions were measured at points positioned throughout the physical model. Measured velocities were then compared with velocities computed using the numerical model. Two bed configurations were used to test the computational model's ability to reproduce the observed flow patterns. The first configuration, designated Plan A lock approach, was simply the river channel in the reach upstream of the lock and dam. The second configuration, referred to as Plan B lock approach, incorporated a series of submerged weirs in the lock approach. Weir fields are used near locks to improve the navigation conditions for tows approaching or leaving a lock. However, placement of weirs in the lock approach produces a complicated bed form that can significantly alter the flow's current magnitudes and directions. Therefore, the weir experiments provided a challenging test of the numerical model's capabilities.

2 Plan A lock approach

Description

The 2-D model was evaluated to determine how well it reproduced the current magnitudes and directions within the Plan A lock approach configuration. Plan A was a river channel approaching the lock and dam, as shown on Figure 3. The contours on Figure 3 are physical model dimensions rather than scaled prototype values. The numerical model simulated the actual physical model dimensions, thereby avoiding scaling issues attributed to differences in Reynolds numbers. The rather simple bathymetry, without submerged weirs, was a good case to test the model's sensitivity to parameters and mesh resolution since the flow patterns are undisturbed in the area upstream of the guard wall.

Figure 3. Plan A lock approach, bed contours.

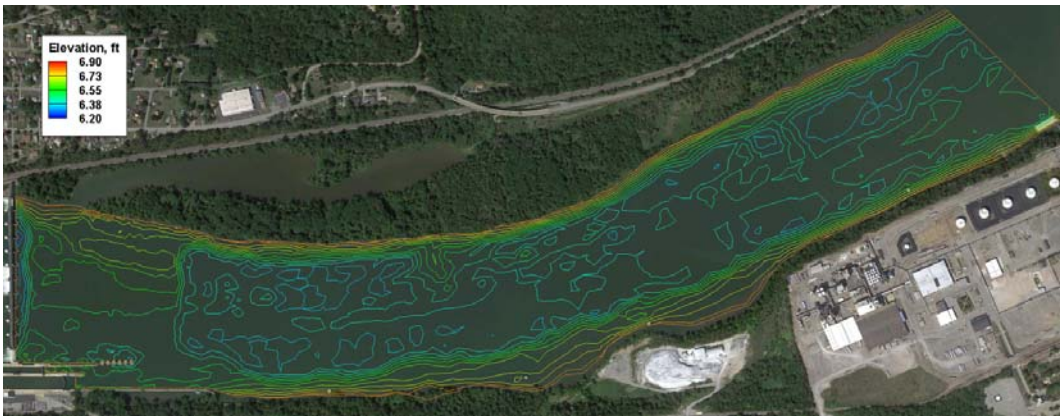

As the flow approaches the guard wall, currents move across the lock approach towards the dam. The dam is a gated spillway that controls the project discharges. Spillway releases direct the current in the upper lock approach toward the spillway. These crosscurrents upstream of the guard wall tend to direct the head of a tow toward the spillway. This flow condition, referred to as outdraft, can cause undesirable navigation conditions.

The outdraft currents are affected by the guard wall configuration, the spillway operation, and the bathymetry of the lock approach. If a numerical model is to be used as a tool to evaluate navigation conditions at lock approaches, it must be able to reproduce the outdraft. Evaluation of the 2-D

model concentrated on the model's ability to simulate velocity magnitude and directions in the flow area near the upper end of the guard wall.

Physical model

The physical model of the Plan A lock approach is shown on Figures 4 and 5. The photographs show that the guard wall consisted of a 4.4-ft-long solid wall and six 0.3-ft-diameter cells spaced 0.5 ft center-to-center. Water was supplied to the model by a pump operating in a circulating system, and the discharge was measured by means of a venturi flow meter. Water-surface elevations were measured with point gages. Velocities at 0.6 depth were measured at points with variable spacing across the navigation channel. Spacing between transects varied from 1.18 ft to 5.56 ft and points along each transect were spaced between 0.50 ft to 2.00 ft apart. Plan A had a total of 11 transects along the navigation channel, as shown in Figure 6. A plan view of the velocity measurement locations is provided in Figure 7. These points were located on the physical model with a total station (digital theodolite and electronic distance meter) and marked for identification as transects along the channel.

Velocity measurement equipment was chosen for minimal water interaction along with setup and data acquisition simplicity. A velocity sensing probe (Nixon Meter) with a measuring head with bladed rotor was selected, as seen in Figure 8. The probe was calibrated for the expected range of velocities.

Figure 4. Photograph of physical model looking from left bank, Plan A lock approach.

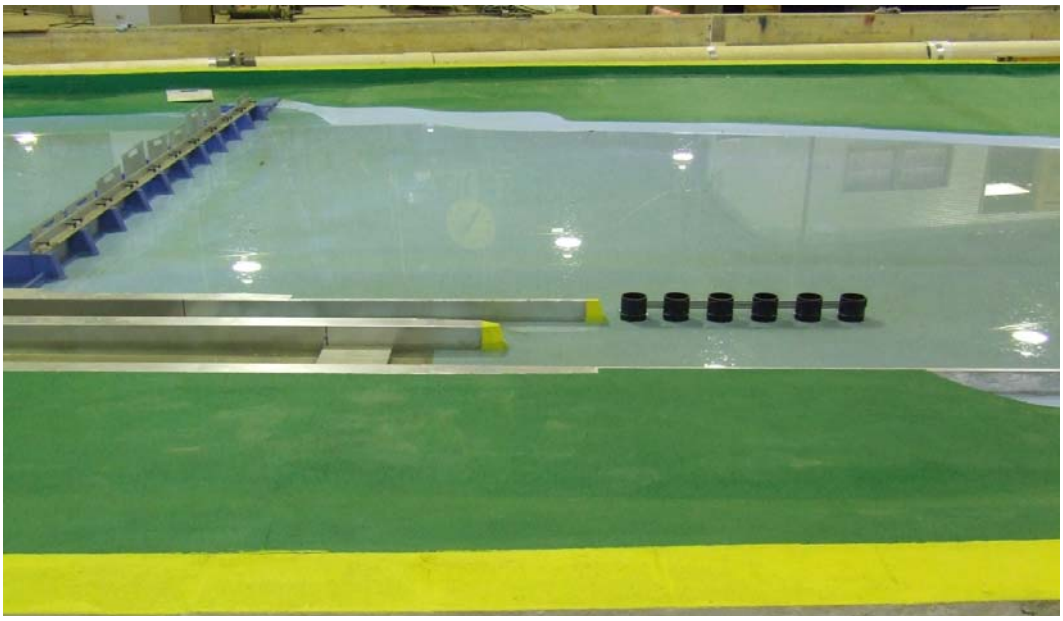

Figure 5. Photograph of physical model looking downstream, Plan A lock approach.

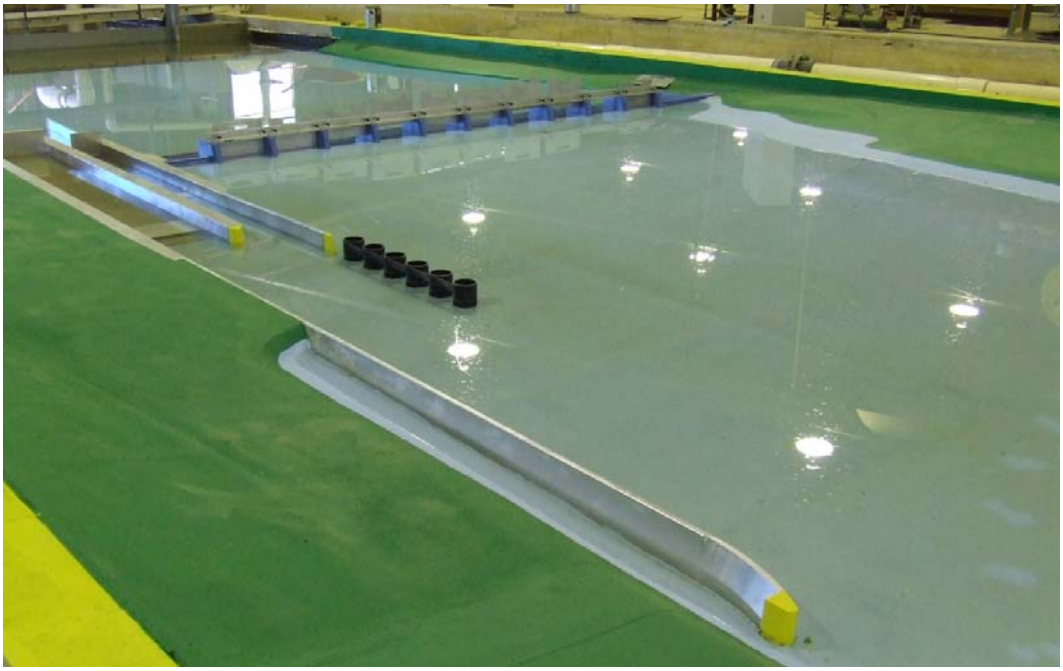

Figure 6. Plan A lock approach, transect layout.

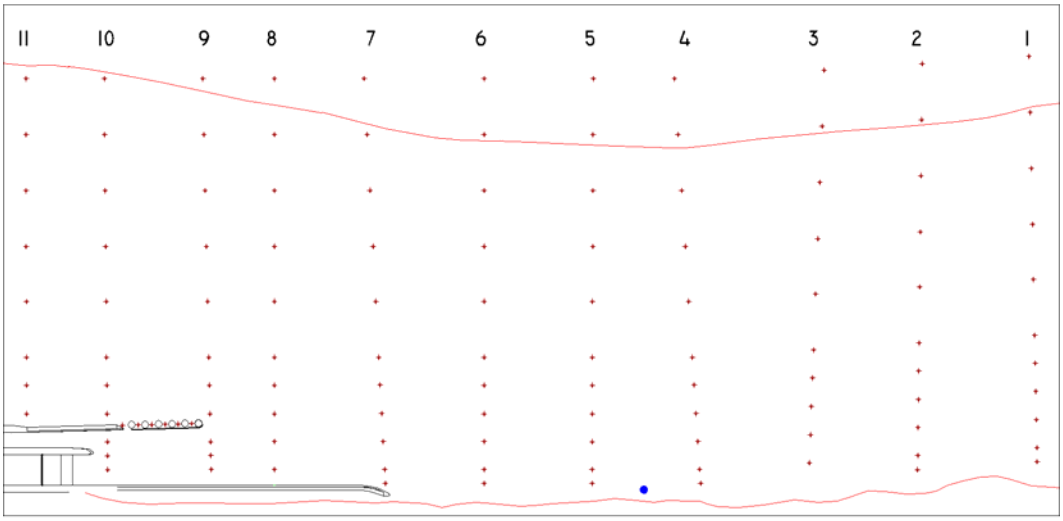

Throughout the grid, the probe was used to measure velocities at points located along the predetermined transects. The probe was placed on a bracket that was fixed to a rail system which was parallel to each transect (Figure 9). The bracket had a graduated scale that allowed measurement of the flow direction (Figure 10). Once the probe was at the desired depth, velocities were measured for a minimum of 2 minutes or until the time-averaged velocity became constant. This process was repeated at each of the marked locations.

Figure 7. Plan A lock approach, layout of velocity measurement locations.

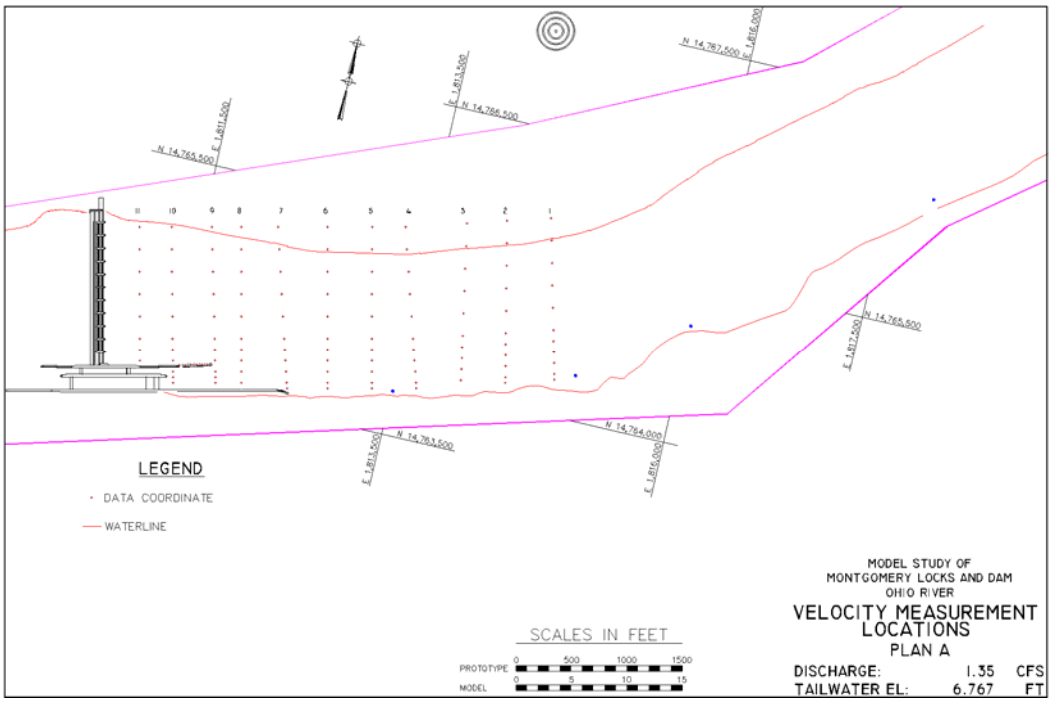

Figure 8. Tools and instrumentation, Nixon meter probe.

Figure 9. Tools and instrumentation, bracket attached to rail.

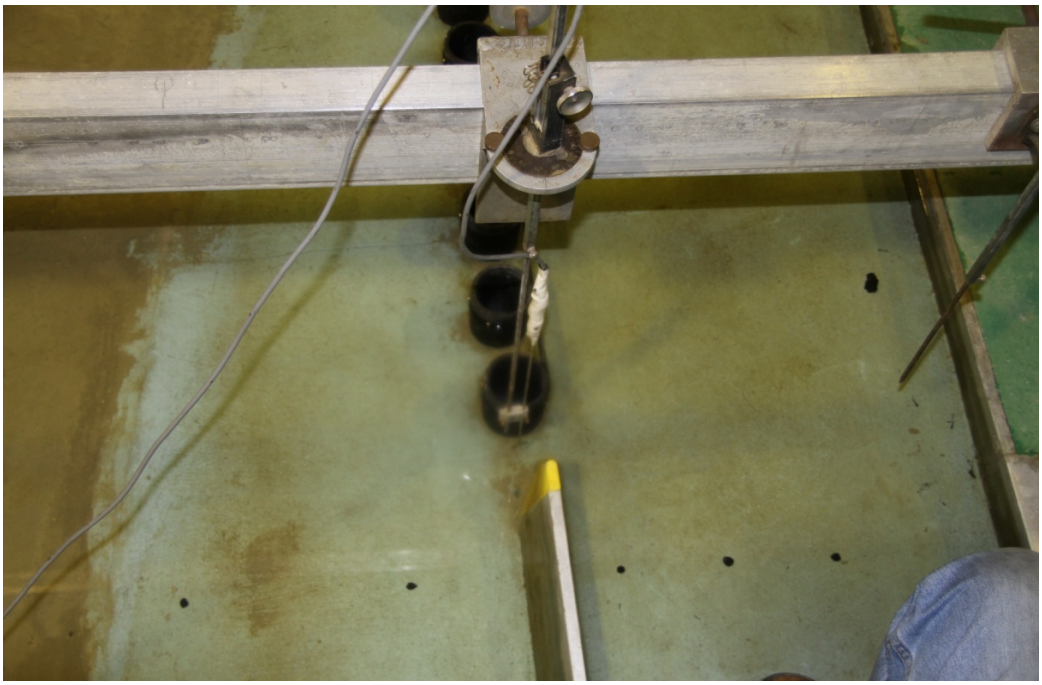

Figure 10. Tools and instrumentation, direction vernier.

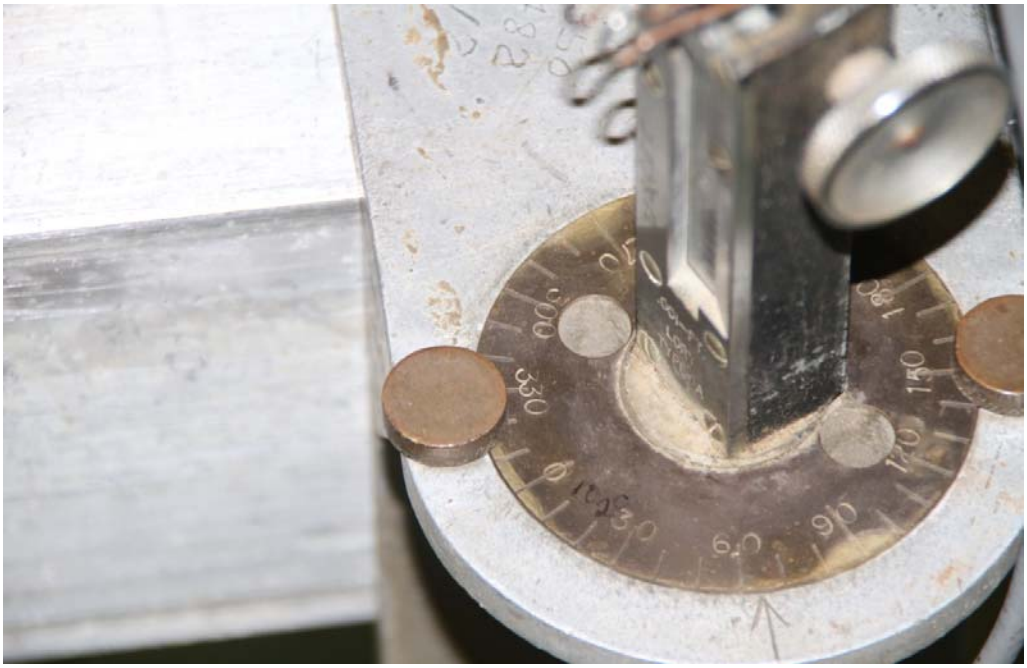

Numerical model

The numerical model is the 2D module of the Adaptive Hydraulics (AdH)[1] finite element flow solver. This code, which was developed by the CHL,

[1] http://adh.usace.army.mil/

features mesh adaption whereby the computational mesh is automatically refined in areas where it is needed to ensure an accurate solution.

The 2D flow model solves the shallow-water equations, which are a result of the vertical integration of the equations of mass and momentum conservation for incompressible flow under the hydrostatic pressure assumption. The flow depth (h), the x-component of velocity (u), and the y-component of velocity (v) define the dependent variables of the fluid motion. The model equations are given as follows:

$$\frac{\partial U}{\partial t}+\frac{\partial F}{\partial x}+\frac{\partial G}{\partial y}+H=0 \tag{1}$$

where:

$$U=\begin{Bmatrix} h \\ uh \\ vh \end{Bmatrix} \tag{2}$$

$$F=\begin{Bmatrix} hu \\ hu^2+\frac{1}{2}gh^2-h\frac{\sigma_{xx}}{\rho} \\ huv-h\frac{\sigma_{yx}}{\rho} \end{Bmatrix} \tag{3}$$

$$G=\begin{Bmatrix} hv \\ huv-h\frac{\sigma_{xy}}{\rho} \\ hv^2+\frac{1}{2}gh^2-h\frac{\sigma_{yy}}{\rho} \end{Bmatrix} \tag{4}$$

$$H = \begin{Bmatrix} 0 \\ gh\dfrac{\partial z_b}{\partial x} + ghS_x \\ gh\dfrac{\partial z_b}{\partial y} + ghS_y \end{Bmatrix} \tag{5}$$

where:

ρ= the fluid density
g= gravitational acceleration
z_b= the channel bed elevation
σ's= the Reynolds stresses due to turbulence plus the molecular stresses, where the first subscript indicates the direction, and the second indicates the face on which the stress acts

$$\sigma_{xx} = 2\rho\nu_t \frac{\partial u}{\partial x} \tag{6}$$

$$\sigma_{xy} = \sigma_{yx} = \rho\nu_t \left(\frac{\partial u}{\partial y} + \frac{\partial v}{\partial x} \right) \tag{7}$$

$$\sigma_{yy} = 2\rho\nu_t \frac{\partial v}{\partial y} \tag{8}$$

where:

ν_t = the sum of eddy and kinematic viscosity
S_x *and* S_y= the friction slope in the x and y directions, respectively

$$S_x = \begin{Bmatrix} n^2 \dfrac{u\sqrt{u^2+v^2}}{C_o h^{1/3}} \\ C_f \dfrac{u\sqrt{u^2+v^2}}{gh^{1/3}} \end{Bmatrix} \tag{9}$$

$$S_y = \begin{Bmatrix} n^2 \dfrac{v\sqrt{u^2+v^2}}{C_o h^{1/3}} \\ C_f \dfrac{v\sqrt{u^2+v^2}}{gh^{1/3}} \end{Bmatrix} \tag{10}$$

where:

n= the Manning's roughness coefficient
C_o= a dimensional constant (C_o = 1 for SI units and 2.208 for US Customary units)
C_f= coefficient of friction.

The equations are discretized using the finite element method in which u, v, and h are represented as linear polynomials on each element.

Computational mesh

The 2D computational mesh was generated using the Surface-water Modeling System (SMS).[1] The bathymetry data used to construct the physical model were also used to create the upstream river bathymetry for the numerical model.

The Plan A mesh, shown in Figures 11-13, consisted of 3,434 nodes and 6,470 triangular elements. It extended about 90 ft upstream from the dam. Element sizes ranged from 0.21 ft by 0.25 ft at the spillway and 0.12 ft by 0.08 ft at the multi-celled guard wall to 0.975 ft by 1.215 ft at the upstream end of the model. Immediately upstream of the dam and in the vicinity of the guard wall, the element sizes were relatively small in order to accurately capture the bed variations. Contours of the bed produced with the computational mesh are shown in Figure 3. Details of the mesh near the spillway and in the vicinity of the guard wall cells are shown in Figures 12 and 13, respectively. The computational mesh resolved each spillway pier as shown in Figure 14. A single material type was used to describe the domain (Figure 15).

Boundary conditions and model parameters

A discharge of 1.35 cfs was set as the inflow boundary condition at the upstream end of the model. The outflow boundary was located at the spillway where flow passed through each gate bay. The crest elevation was 6.67 ft, and the outflow boundary condition was a water-surface elevation of 6.82 ft. The model was run from initial conditions of a quiescent pool at a 6.832-ft water-surface elevation to steady state by advancing in time until the solution did not vary with additional time steps. The initial pool elevation was higher than any computational node's elevation ensuring that the initial depth at each node was a positive value.

[1] http://chl.erdc.usace.army.mil/sms

Figure 11. Plan A lock approach, upstream approach computational mesh.

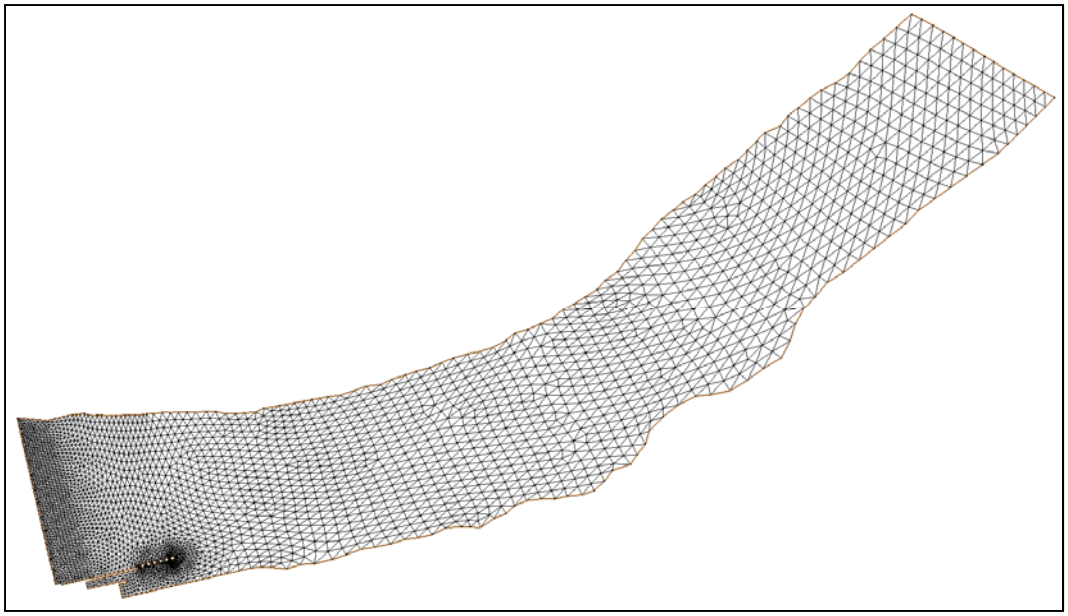

Figure 12. Plan A lock approach, detailed view of computational mesh near lock and dam.

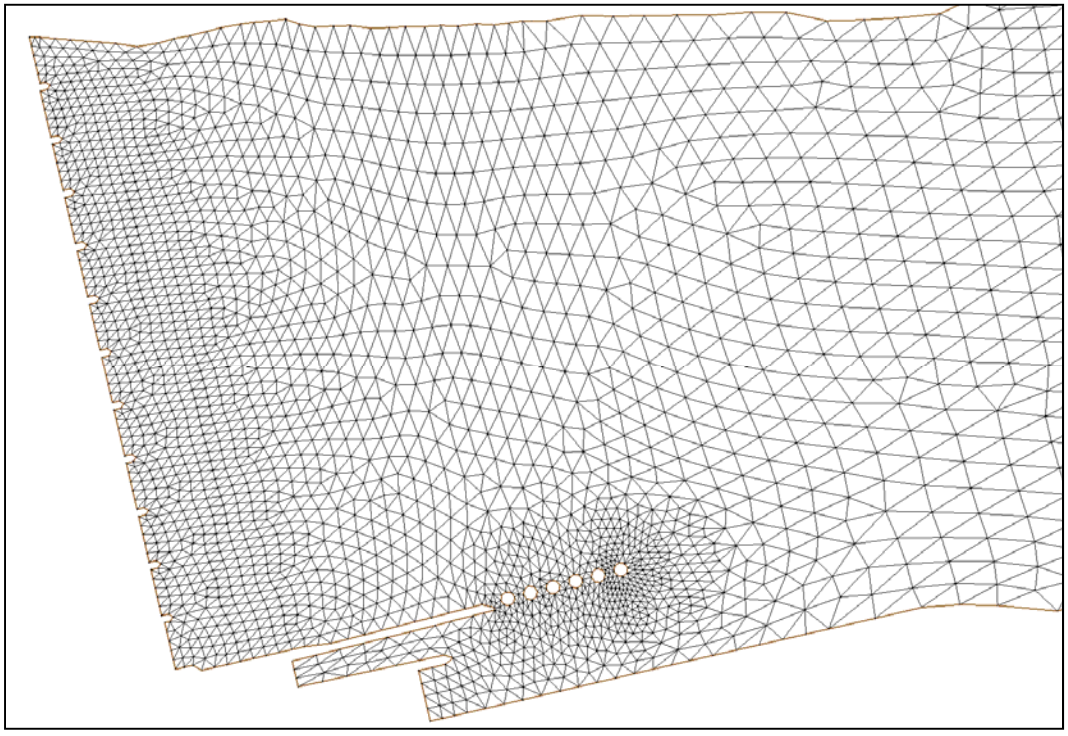

Figure 13. Plan A lock approach, detailed view of computational mesh near lock guard wall.

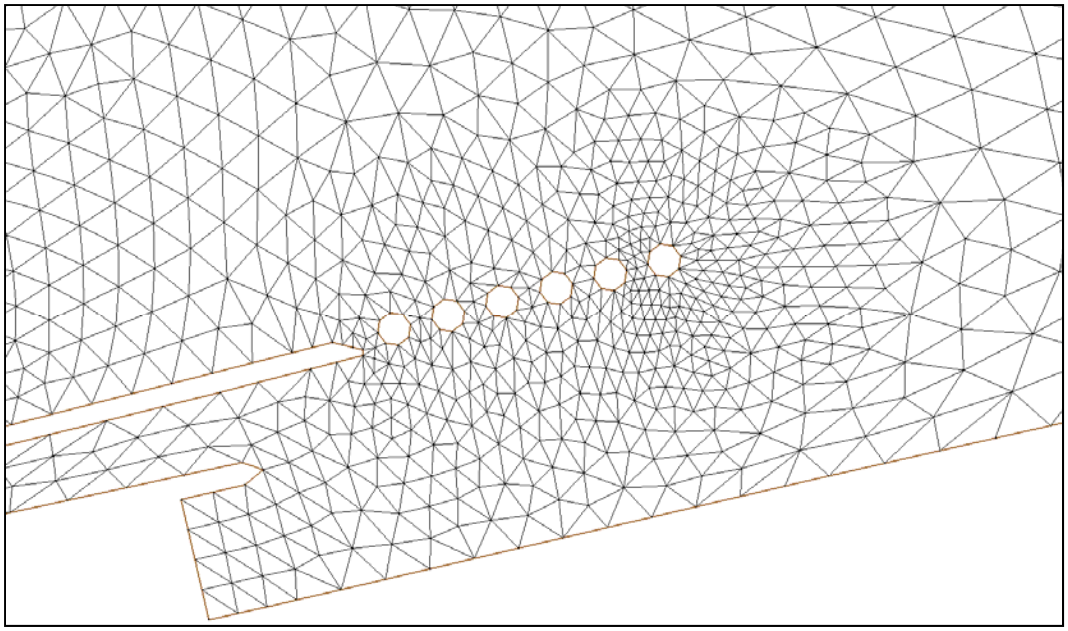

Figure 14. Plan A lock approach, detailed view of computational mesh near spillway piers.

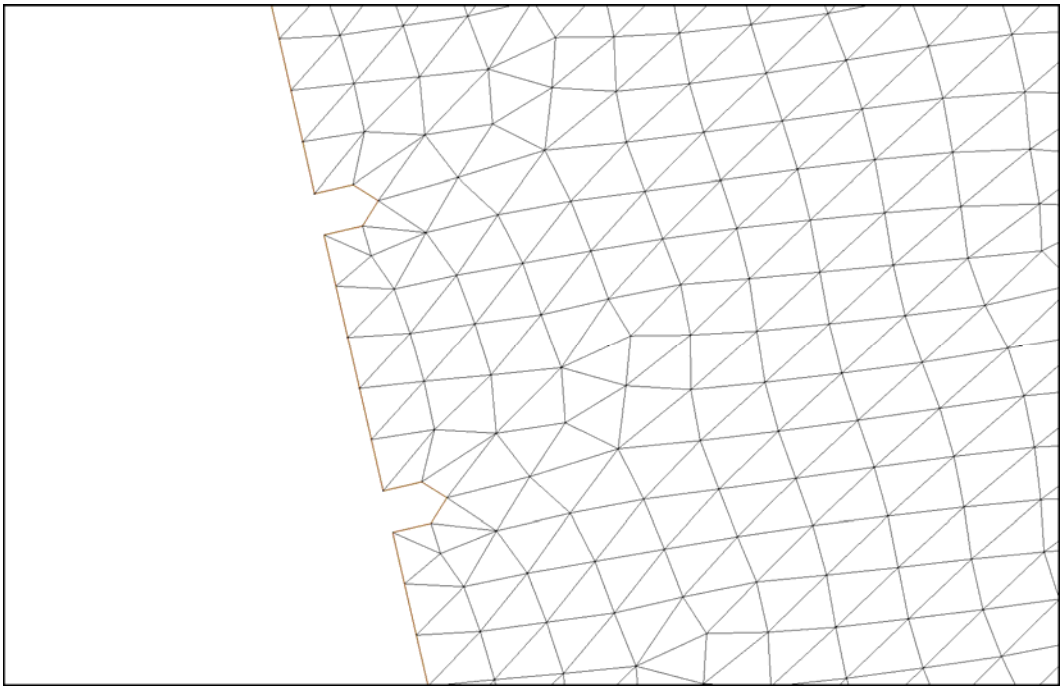

Figure 15. Plan A lock approach, upstream approach material distribution.

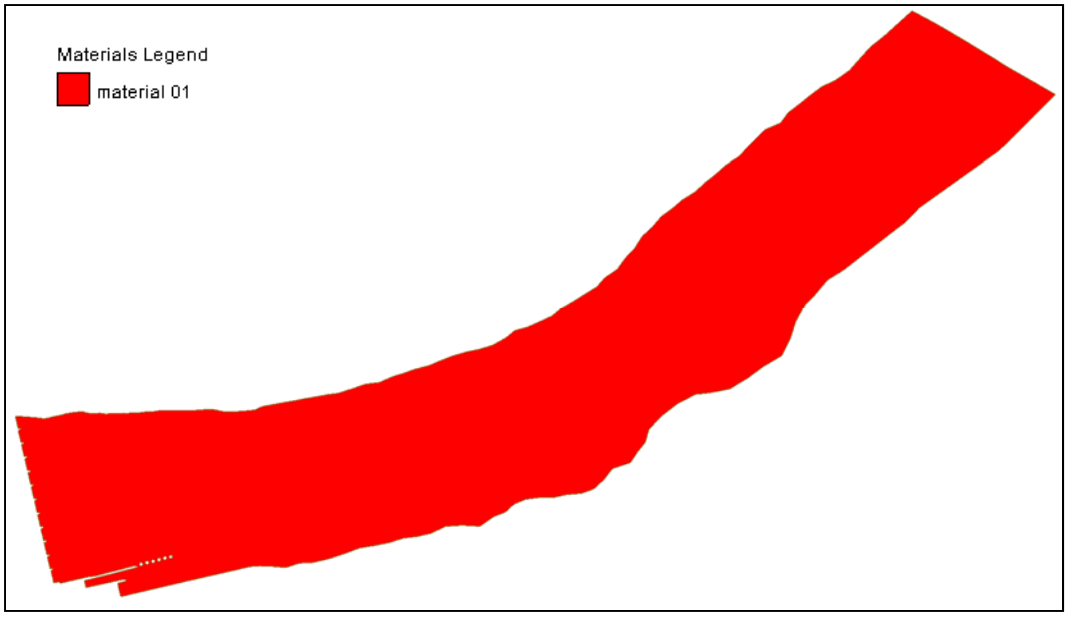

Eddy Viscosity and Bed Roughness

The stress terms in the governing equations are a sum of molecular shear and Reynolds, or turbulence, stresses. The viscosity (ν_t) is the sum of the kinematic viscosity of water and the eddy viscosity (ε). The eddy viscosity is used to calculate the turbulence stresses which model the effects of turbulent mixing. Two separate eddy viscosity terms were used, an isotropic term that accounts for turbulent mixing:

$$\varepsilon_I = 0.92k\sqrt{C_d}hU \tag{11}$$

and an additional anisotropic term in the direction of flow that accounts for stream wise dispersion:

$$\varepsilon_A = 1.3\sqrt{C_d}hU\,. \tag{12}$$

where:

k = a user-defined scaling coefficient
C_d = the drag coefficient, as determined by the bed friction
U = the depth-averaged velocity.

Numerical model results

Initial evaluation of the model parameters, Manning's n and the k coefficient, was conducted without mesh adaption. Manning's n values ranging from 0.012 to 0.015 were used to model the roughness of the physical model's brush-finished concrete bed. The k coefficient was varied from 0.3 to 0.7. The scaling coefficient, k, had an effect on the velocity distribution. Velocities calculated using smaller k coefficient values were consistently more accurate in reproducing observed velocities.

Automatic mesh refinement was used to achieve mesh convergence. The mesh was converged by advancing in time from the original mesh's steady-state solution to steady-state solutions with one and two levels of adaption. The solution with two levels of adaption did not significantly differ from the solution obtained with one level of adaption. The difference in the velocity magnitudes computed using two levels of adaption did not differ from those obtained with 1 level of adaption by more than 0.02 fps.

Plan A results

An inflow of 1.35 cfs was introduced at the upstream limit of the physical model. The inflow passed through a baffle made of rubberized bound fiber. Piezometers were installed along the channel thalweg to monitor and adjust the water-surface elevation as needed.

Adjustable plates were used to simulate various gate openings in each of the ten spillway gates. The spillway was operated such that the two bank-side gates and two lock-side gates were opened 0.76 inches, and the remaining gates were opened 0.9 inches.

The measured velocities are shown as vectors in Figure 16. The velocity vectors show that the flow was fairly uniform as the flow moves down-stream. Generally, the lateral variation was similar across each of the seven most upstream transects. The uniformity was due to the constant cross-sectional shape. The flow in the navigation lane near the left descending bank accelerated as it neared the guard wall. The flow velocity between the piers is about 2.9 fps.

The flow rotated slightly through the channel's natural curvature as it approached the guard wall cells. A slight channel contraction occurred on the left descending bank upstream of the lock approach. The flow between

transects 8 and 9 had a small change in direction compared to previous transects. Around transect 8, the flow contracted in the vertical direction. This vertical contraction increased the velocity as seen in Figure 16. The guard wall cells restricted the horizontal area and forced the flow to change direction toward the spillway. This change can be seen in the vectors on the last four transects. The calculated flow distribution is illustrated by the velocity magnitude contours on Figure 17.

Figure 16. Plan A lock approach, physical model velocities.

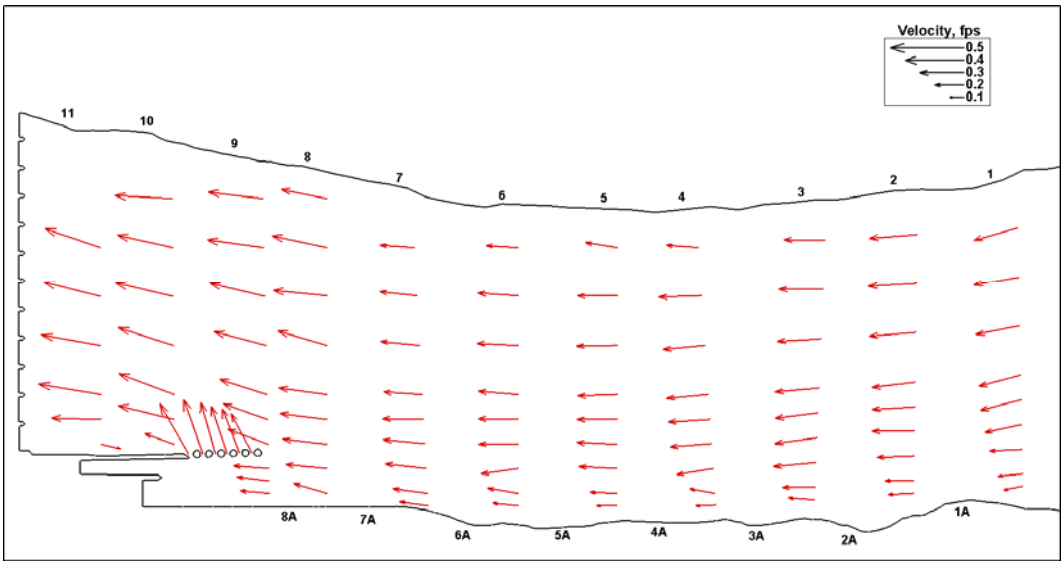

Figure 17. Plan A lock approach, computed velocity magnitude contours, k = 0.7, n = 0.013; 2 levels of adaption.

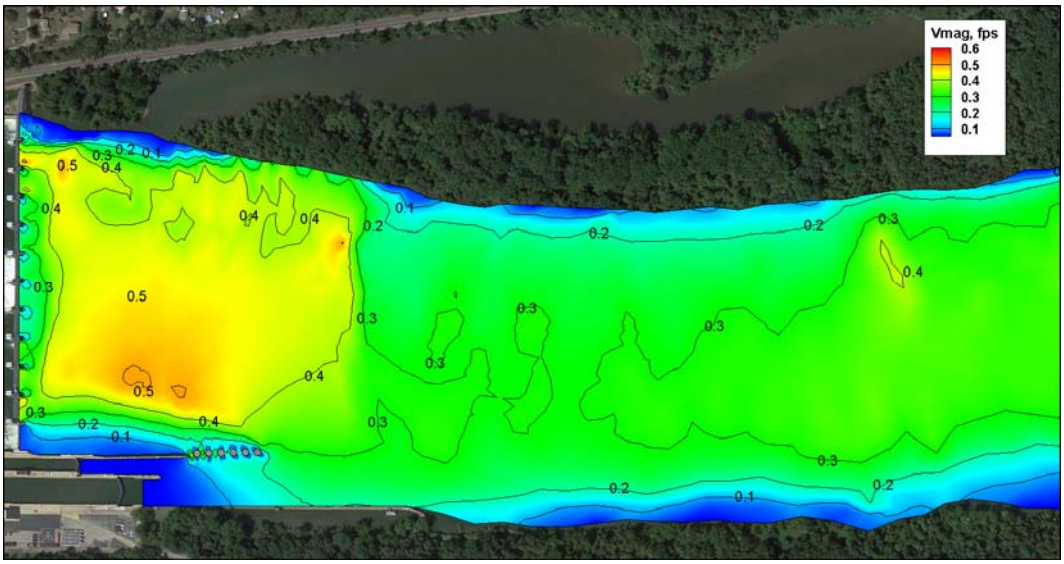

The measured and calculated flow patterns for this bathymetry are illustrated in Figure 18. The measured and calculated velocities did not differ significantly throughout the channel. However, approaching the lock and dam, the calculated velocities differed slightly from the measured values. This difference is relatively negligible and the vector magnitudes and directions were similar.

Figure 18. Plan A lock approach, physical model data (red) & numerical model results, k = 0.7, n = 0.013 (black).

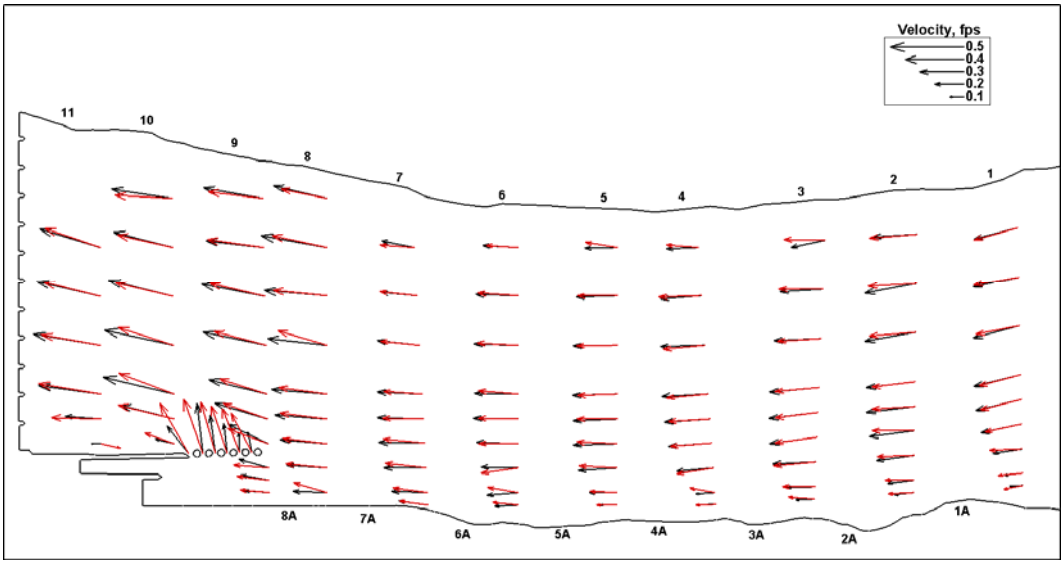

The computed flow distribution between the guard wall cells was more uniform than the distribution observed in the physical model. The velocity vectors shown in Figure 18 illustrates that the calculated flow direction was more orthogonal to the guard wall than the direction observed in the physical model. Also, the calculated velocity magnitude was smaller than the observed velocity.

Another method of comparing the measured and calculated velocity distribution, in addition to the velocity vectors shown in Figure 18, consists of plotting contours of differences in velocity magnitudes. The difference in measured and calculated velocity magnitude (E) is defined as follows:

$$E = V_m - V_c \tag{13}$$

where:

V_m and V_c = the measured and calculated velocity magnitudes, respectively. The velocity magnitudes are

$$V_i = \left[u_i^2 + v_i^2\right]^{1/2} \tag{14}$$

where the subscript i refers to either the measured (m) or calculated (c) values.

The differences in measured and calculated velocity magnitudes ranged from 0.186 fps to -0.093 fps. The largest differences occurred at the sudden change in bed slope between transects 8 and 10 and in the flow between the guard wall cells. The calculated velocity differed from the measured velocity less that 0.05 fps over a major portion of the flow field (Figure 19).

Figure 19. Plan A lock approach, contours of difference in measured and calculated velocity magnitude, *E*.

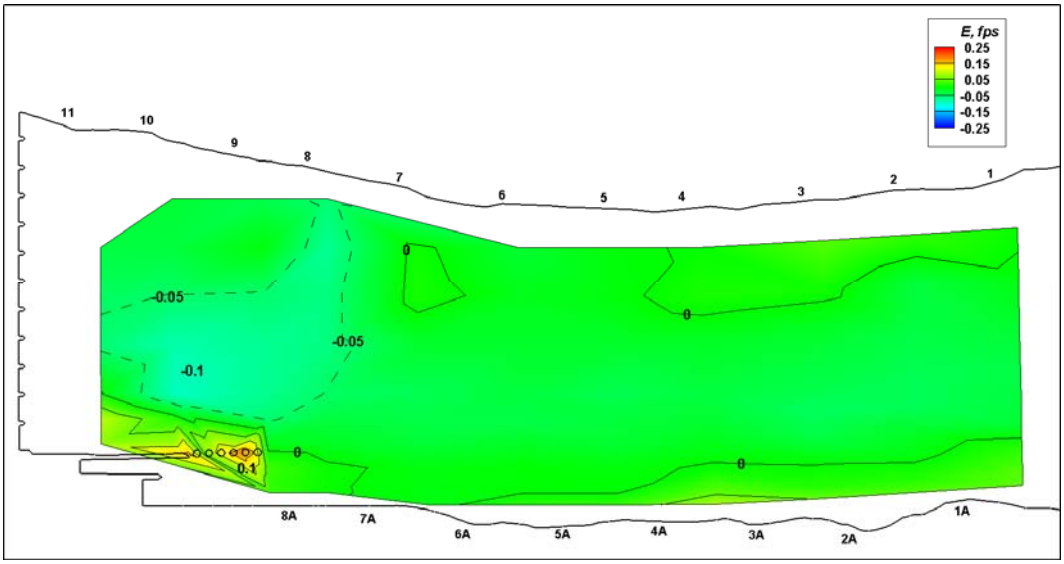

There are several possible reasons for the differences in the measured and calculated velocity magnitudes. One reason may be due to the assumption that the depth-averaged velocity occurs at 0.6 depth, which is where the single velocity was measured in the physical model. The 0.6 depth assumption is reasonable for regions where the flow is fully established but is not for areas where the flow is accelerating, especially where vertical accelerations are significant such as in the vicinity of the guard wall cells.

Not only is the 0.6 depth assumption for the vertical position where the velocity equals the depth-averaged velocity unreasonable in the vicinity of the guard wall cells, the equations solved by the 2D numerical model do not represent an important flow feature (vertical acceleration) in this area.

The hydrostatic pressure assumption of the model equations results in over prediction of the runup on the upstream side of piers and excessive drawdown on the downstream side. So, the computed water-surface differential across the pier is larger than the change observed in the real system. However, this is only a local error because the numerical model conserves momentum and is applicable for most of the flow field which is hydrostatic.

3 Plan B lock approach

Description

The second design, Plan B lock approach, had a series of submerged weirs constructed normal to the flow direction. The weirs were abutted to the left descending bank as shown in Figure 20. The bed configuration of Plan B is shown in Figures 21 through 23. Figure 23 shows that the weirs extended as much as 4.9 ft into the river. A typical weir cross section is shown in Figure 24. The weirs were designed to reduce velocities in the lock approach by means of training the flow toward the main channel.

Physical model

The physical model of the Plan B lock approach is shown in Figure 20. The weirs were positioned such that azimuths of their directions varied. The presence of the weirs in the lock approach retards the flow in the lock approach and can have an effect on the water-surface elevation in the reach. However, this water-surface change was not large enough in the physical model to be measured with the piezometers.

Velocities were measured at 0.6 depth at the same points where Plan A velocities were measured and along additional transects that were positioned on and parallel to each weir. The distance between data points ranged from 0.5 to 1.0 ft over the weirs and 2.0 ft throughout the main channel. The velocity measurement points are shown in the general layout in Figure 21 and the detailed sketch in Figure 22.

Computational mesh

The Plan B mesh, shown in Figure 25, consisted of 7,659 nodes and 14,787 triangular elements, which was more than double the mesh density used to model Plan A. Element sizes ranged from 0.015 ft by 0.067 ft at the weir, 0.053 ft by 0.114 ft at the multi-celled guard wall, and 0.975 ft by 1.215 ft at the upstream end of the model. Throughout the weir field, the element sizes were required to be relatively small to capture the features of the bed topography. Details of the mesh in the vicinity of the weirs are shown in Figures 26 and 27. Contours of bed elevations are shown in Figure 28. A material type was assigned for the weirs separate from the rest of the model domain (Figure 29).

Figure 20. Plan B lock approach looking upstream, weir field on left descending bank.

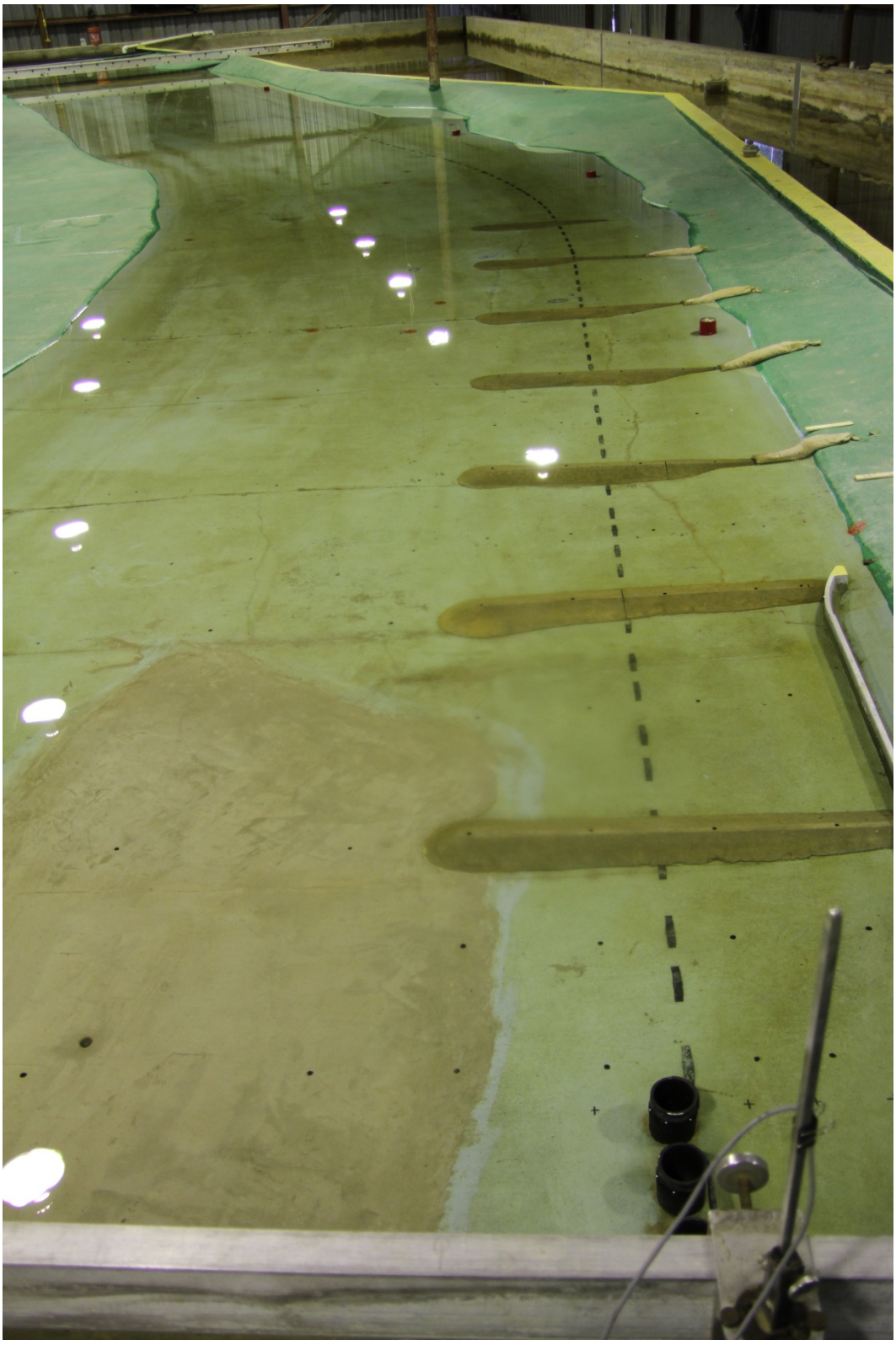

Figure 21. Plan B lock approach, layout of velocity measurement locations.

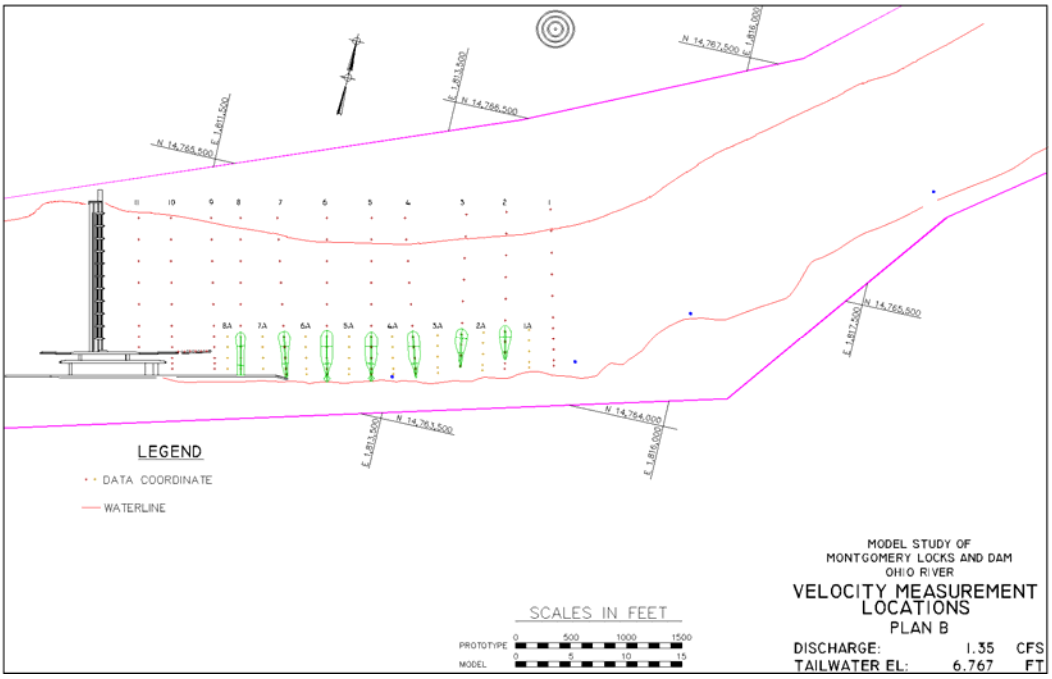

Figure 22. Plan B lock approach transect layout.

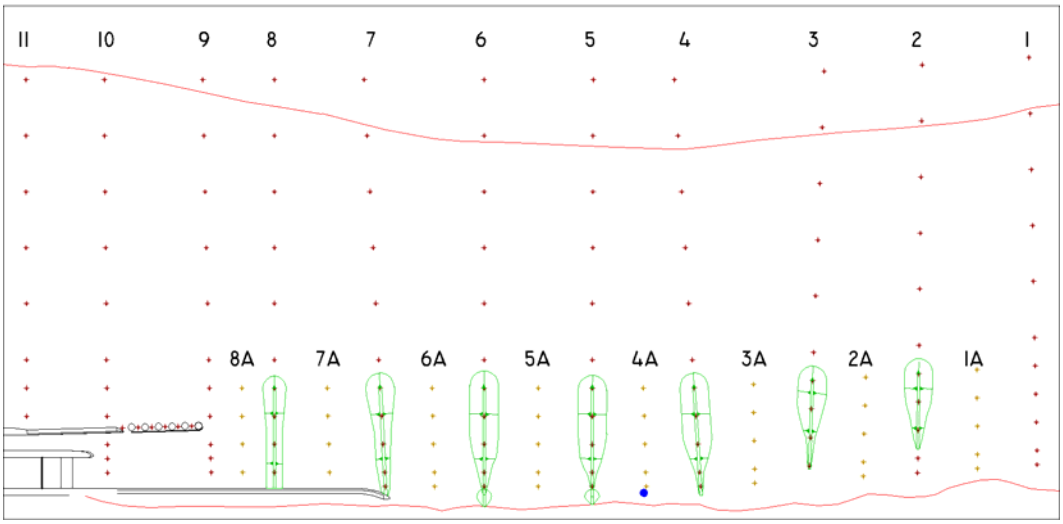

Figure 23. Plan B lock approach, weir lengths, distances from waterline.

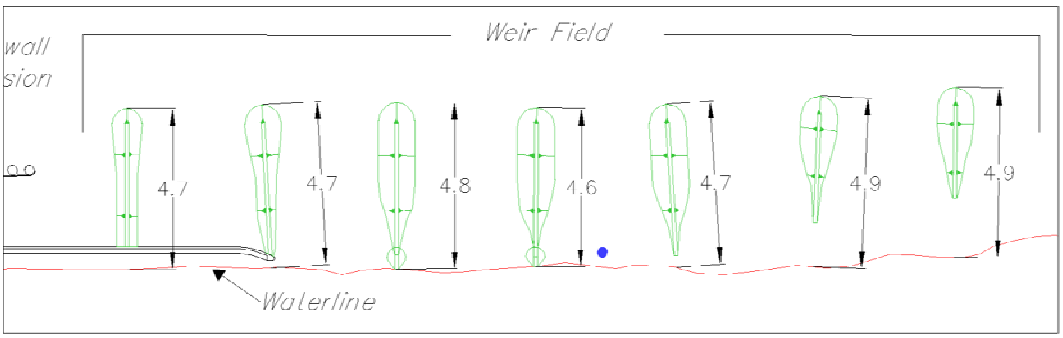

Figure 24. Plan B lock approach, typical weir.

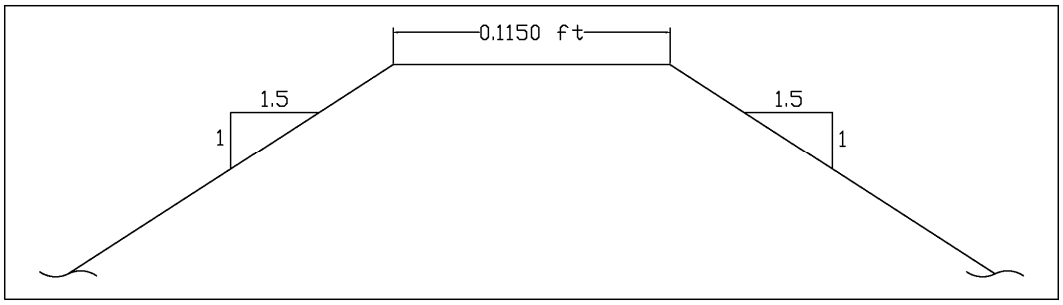

Figure 25. Plan B lock approach, upstream approach computational mesh.

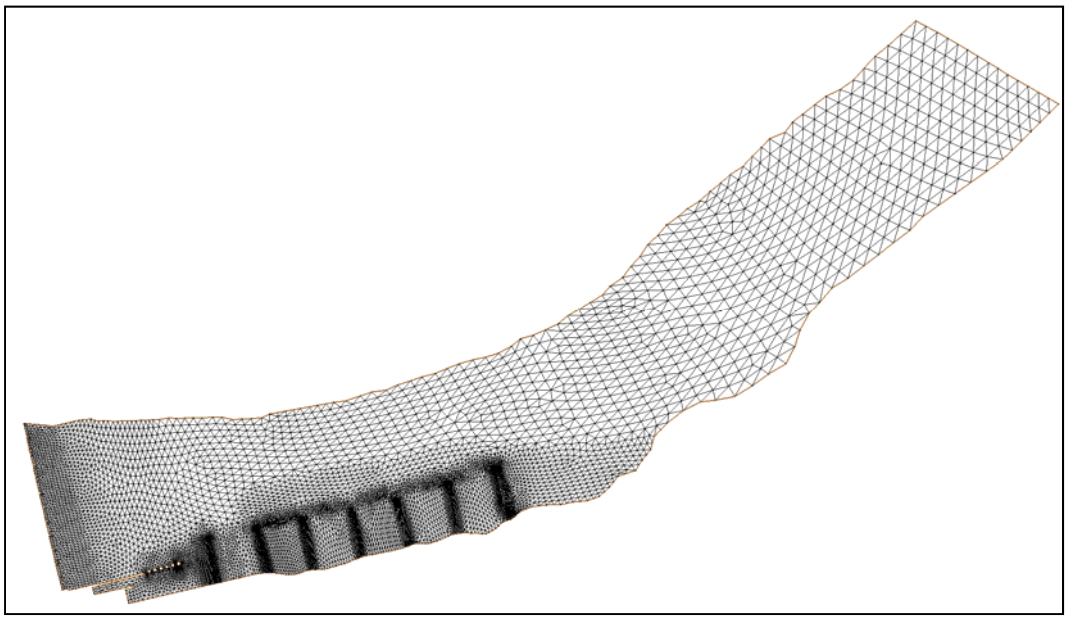

Figure 26. Plan B lock approach, detailed view of computational mesh of weir field.

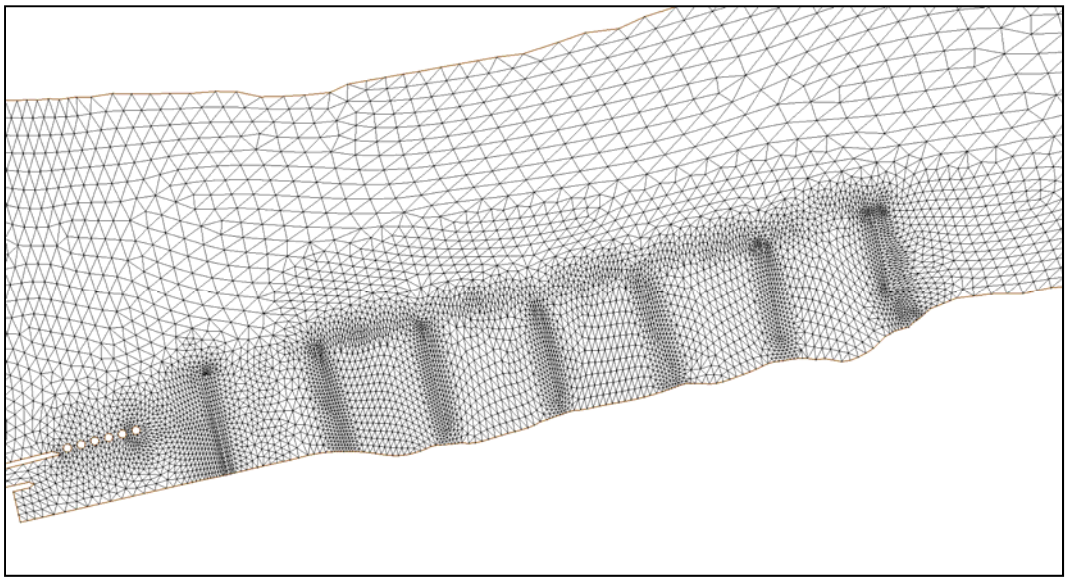

Figure 27. Plan B lock approach, detailed view of computational mesh near lock guard wall.

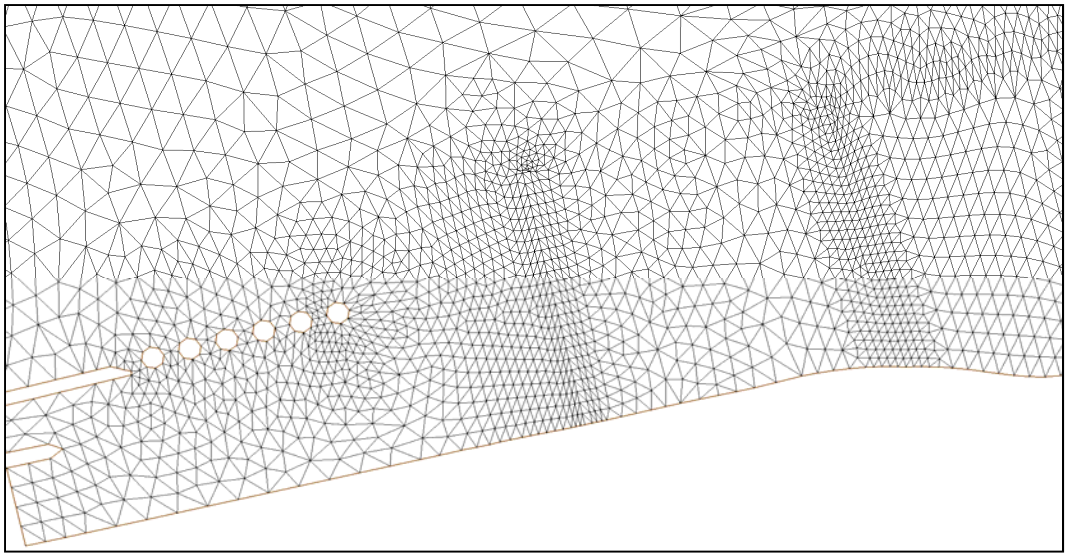

Figure 28. Plan B lock approach, channel bed contours.

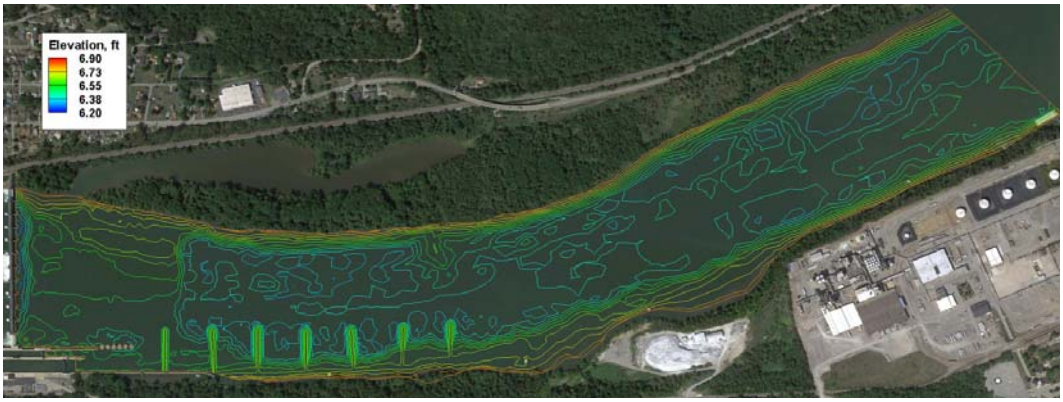

Figure 29. Plan B lock approach, upstream approach material distribution.

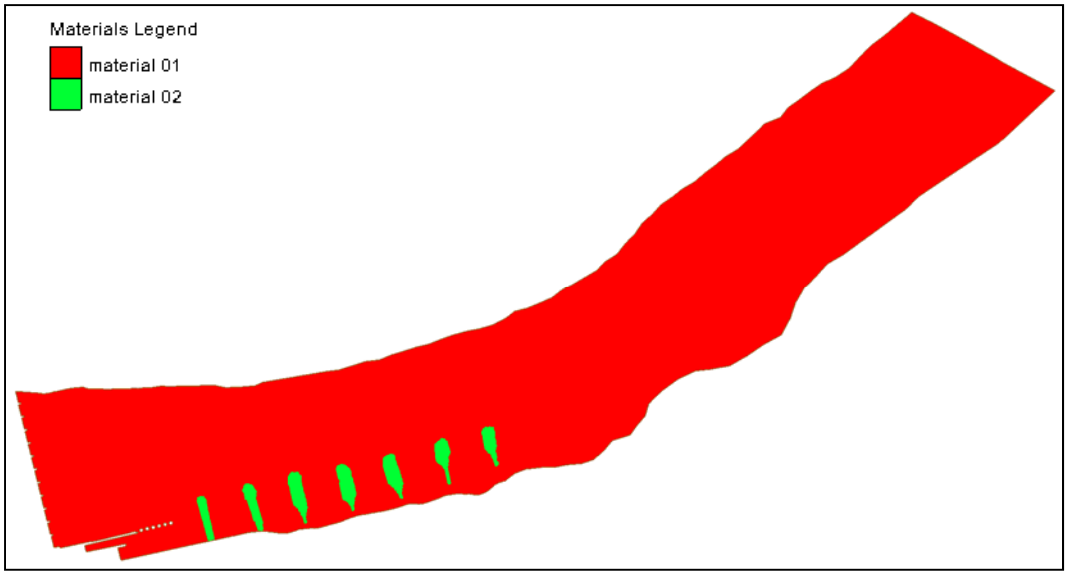

The computational mesh was converged using automatic mesh refinement. However, after initial mesh refinement, further refinement did not produce significantly different velocity vectors for constant n and k values.

Boundary conditions and model parameters

The flow setup and gate settings for Plan B were identical to the Plan A experiments. The discharge introduced at the upstream boundary was 1.35 cfs and flow exited the model at the spillway where the two gates on the right end and two gates on the left end of the spillway were set to 0.76 inches open, and the remaining gates were set to 0.9 inches open.

Numerical modeling of flow over submerged weirs using depth-averaged hydrostatic equations is complicated by the fact that the flow is not fully developed and that the pressure distribution is not hydrostatic near the upstream edge of the weir crest. Both the effective bed roughness and the turbulent momentum diffusion affect the computed velocity magnitude and direction. Yet, appropriate coefficients needed to model a series of weirs are not known.

Plan B results

The scaling coefficient, k, which is used to estimate the Reynolds stresses caused by turbulence, and the Manning's roughness coefficient, n, had a significant effect on the computed velocities. For a reasonable range of Manning n values, larger k coefficients provided velocities that better represented the measured velocities. The use of a smaller Manning's roughness coefficient resulted in increased agreement between the calculated and the observed velocities.

The velocity in the physical model was observed to vary in magnitude and direction, particularly in the flow over the weir field (Figure 30). The velocities at the weir crests were measured at transects 2 through 8 (Figure 21). The flow contracts and accelerates as it passes over each weir. The velocity of the flow between each weir was measured at transects 2A through 7A (Figure 22). The flow at these transects is deeper, so the velocity is slower than at the weir crests. These velocity changes are shown on the vector plot of physical model data in Figure 30.

The flow distribution with the Plan B approach, computed with the 2D numerical model, is illustrated in Figure 31. The depth-averaged velocity magnitude contour plot in Figure 31 shows that the weirs retard the flow.

Figure 30. Plan B lock approach, physical model results.

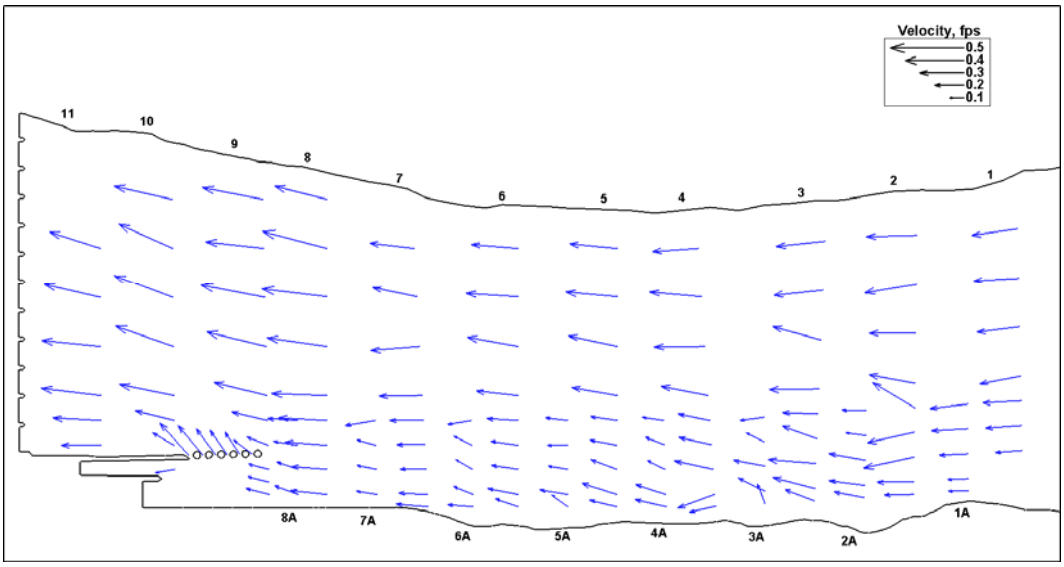

Figure 31. Plan B lock approach, computed velocity magnitude contours, k = 0.7, n = 0.013; 2 levels of adaption.

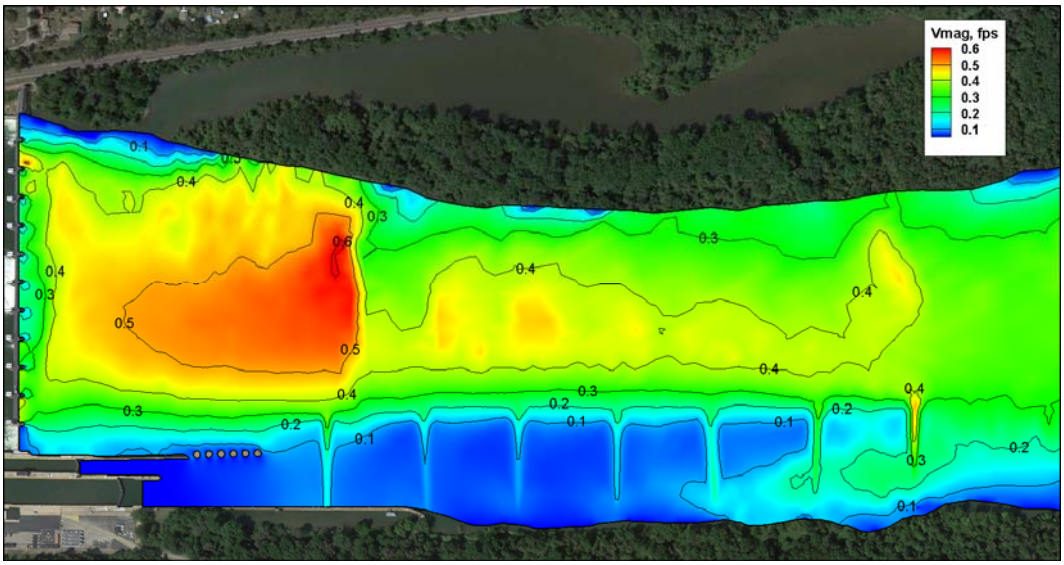

This velocity reduction is the weirs' design objective. The weirs decrease the velocity across the weir field, thereby improving the navigation conditions for tows approaching the lock. The velocity reduction not only lowers outdraft at the wall's end but also provides conditions for better tow boat steerage.

Velocity vectors from the measured data and calculated results are plotted together in Figure 32. This vector plot shows that the changes in measured velocity magnitude, as flow passes over and between the weirs, is not as pronounced in the numerical model results. Some of this difference is

attributed to the fact that the velocity, measured at a single point in the flow column, was assumed to represent the average value over the depth at that point.

Figure 32. Plan B lock approach, physical model data (blue) and numerical model results, k = 0.7, n = 0.013 (black).

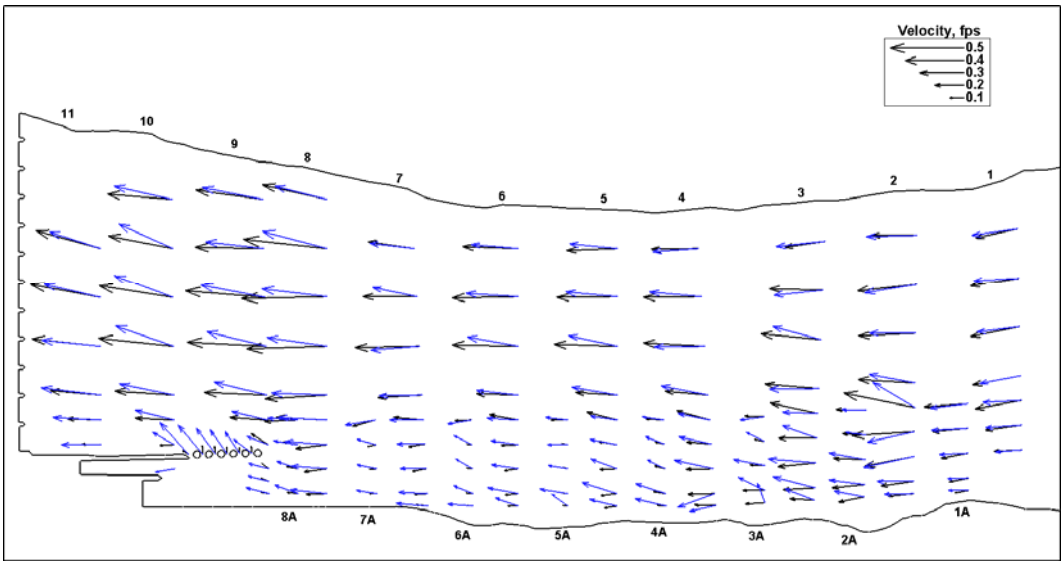

The direction of the computed flow over the weir field was different than the direction observed in the physical model. The numerical model results show flow in the longitudinal direction across the entire weir field, whereas the physical model flow directions, although variable, generally had a lateral component toward the main channel. Also, the velocity of the flow between the guard wall cells in the physical model exerted lateral momentum on more than half of the width of the main channel flow. The calculated velocity between the guard wall cells was not large, and the lateral momentum was not sufficient to affect the main channel flow direction (Figure 32).

Differences in the measured and calculated velocity magnitudes, E, are plotted as contours in Figure 33. The measured velocities were consistently larger than the calculated values within the flow over the weir field. Within the main channel flow, the measured velocities were smaller than the calculated values. Additionally, vector orientations over the weirs and in the dam approach were different. The calculated velocity magnitudes and directions of flow between the guard wall cells differed significantly from the measured values. Differences in measured and calculated velocity magnitudes ranged from 0.239 fps to -0.155 fps.

Figure 33. Plan B lock approach, velocity magnitude difference, *E*.

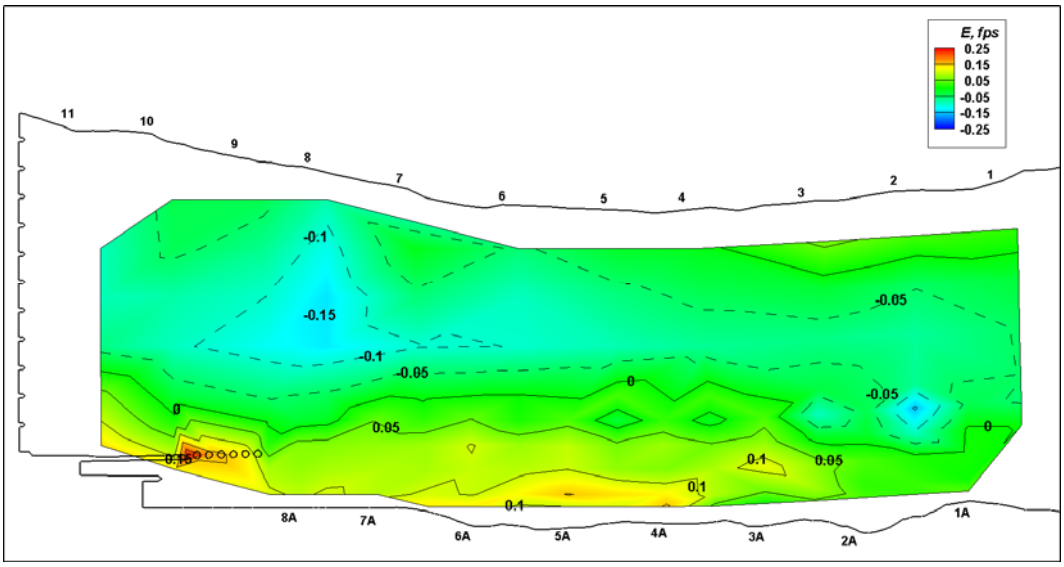

Measurement of the *depth-averaged* velocity was difficult because the flow over each weir was shallow. The velocity probe was approximately one-half inch in diameter, and the flow depth at the crests of the weirs was about 0.15 ft. So, the probe occupied about one-fourth of the flow depth at the weir crests. Also, the velocity at 0.6 depth is reasonably close to the depth-average value for fully developed, uniform flow. However, the flow over the weir field is far from uniform, and the vertical velocity distribution is not known.

The difference with 2D depth-averaged numerical model results in the Plan B is thought to be a combination of sudden reduction in water depth approaching each weir and the dam approach. The contraction of the water depth over the weir is designed to be 0.15 ft. The bathymetry approaching the dam has an increase in elevation ranging from 0.08 ft to 0.20 ft. The numerical model assumes hydrostatic pressure distribution wherein the inertia in the vertical direction is negligible. The sudden vertical contraction in the bathymetry causes a velocity gradient that is not captured in the equations, causing discrepancies with measured data.

Weir modeling experiments

Numerical experiments were conducted to determine if the weir field effects could be better represented by the numerical model. The mesh was converged and velocities did change after initial refinement. Additional refinement did not significantly change velocities, indicating that mesh resolution was not an issue. Simulations were completed with the Manning's *n* for the

weirs varying from 0.008 to 0.010 and 0.013 for the remainder of the flow domain. A Manning's n of 0.008 for the weirs significantly increased velocities over the weirs (Figure 34); however, the increase was too large. Flow between the guard wall cells also increased, yet remained significantly smaller than the measured velocities. The velocities calculated using a Manning's n value of 0.010 for the weirs and 0.013 for the remainder of the model are shown in Figure 35. The calculated velocities resulting from a Manning's n of 0.010 were almost identical to those calculated using a n of 0.013 (Figure 35).

Figure 34. Plan B lock approach, physical model data (blue) and numerical model results, k = 0.7, n = 0.008 (black).

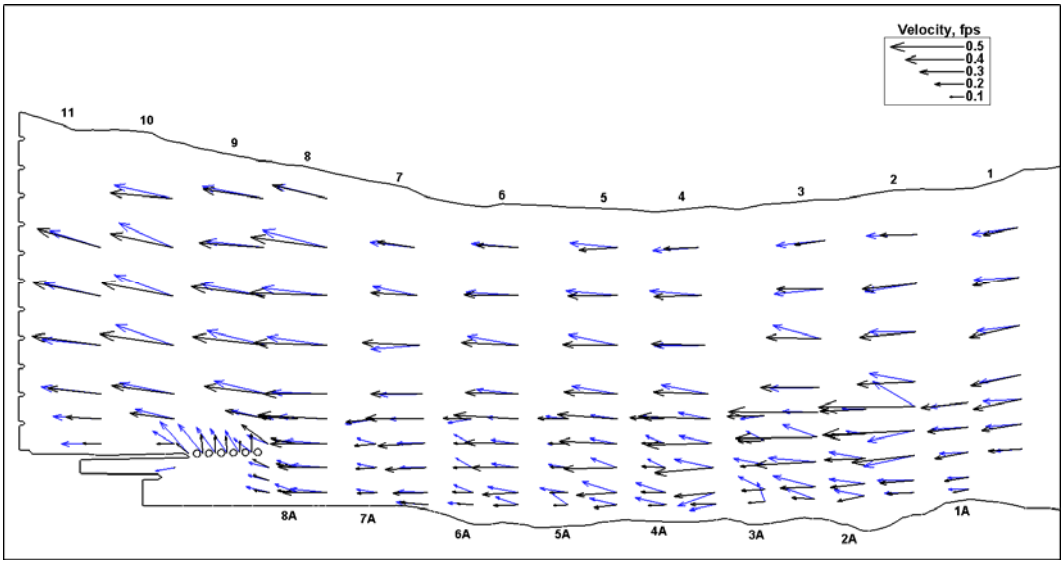

Figure 35. Plan B lock approach, physical model data (blue) and numerical model results, k = 0.7, n = 0.010 (black).

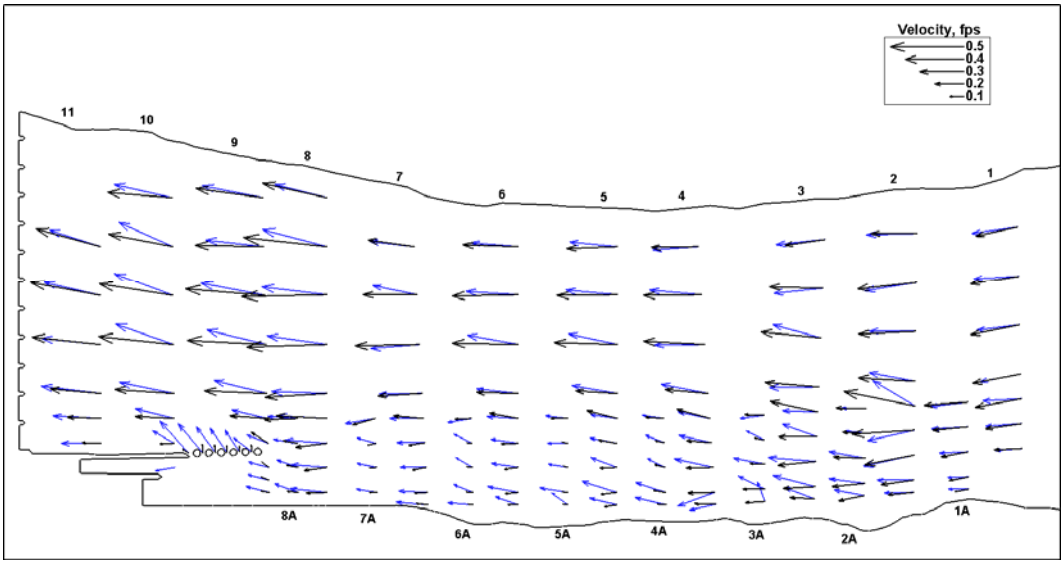

The material used to identify the bed friction roughness coefficient for the weirs was extended upstream from each weir about one weir width (Figure 36). Simulations were completed with the Manning's n for the weirs of 0.008, 0.010, 0.014, and 0.024. The Manning's n for the remainder of the flow domain was 0.013. The computed velocities resulting from extending the weir material with Manning's n values of 0.008, o.010, 0.014, and 0.024 are compared to physical model data in Figure 37 through Figure 40, respectively. Lower roughness coefficients resulted in flow concentration over the weir field. Flow through cell walls increased, and the direction was no longer orthogonal to the guard wall.

In an attempt to better reproduce data over the first weir in the lock approach, a larger Manning's n value for the weirs was specified. The larger roughness coefficient caused the flow to follow the main channel and significantly reduced the flow over the weir field. Flow between the guard wall cells was reduced as well. Compared to previous solutions, there was no significant change in velocities. Differences were primarily found in the vicinity of the upstream end of the weir field at transect 2.

Figure 36. Plan B lock approach, upstream approach material distribution with extended weir material.

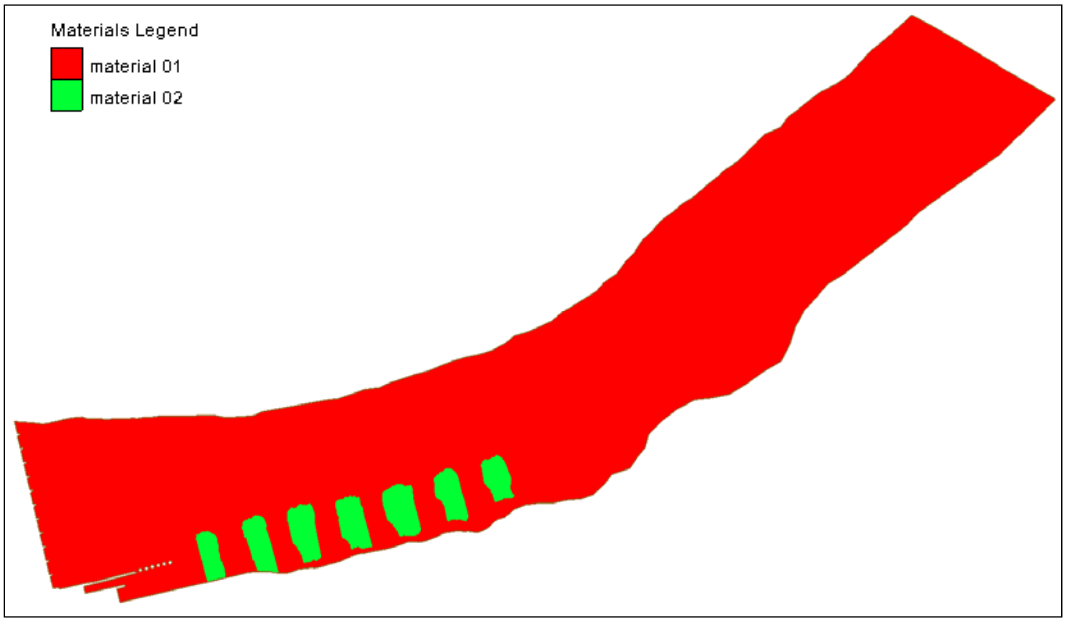

Figure 37. Plan B lock approach, extended weir material, *n* = 0.008, physical model data (blue), and numerical model results, *k* = 0.7, *n* = 0. 008 (black).

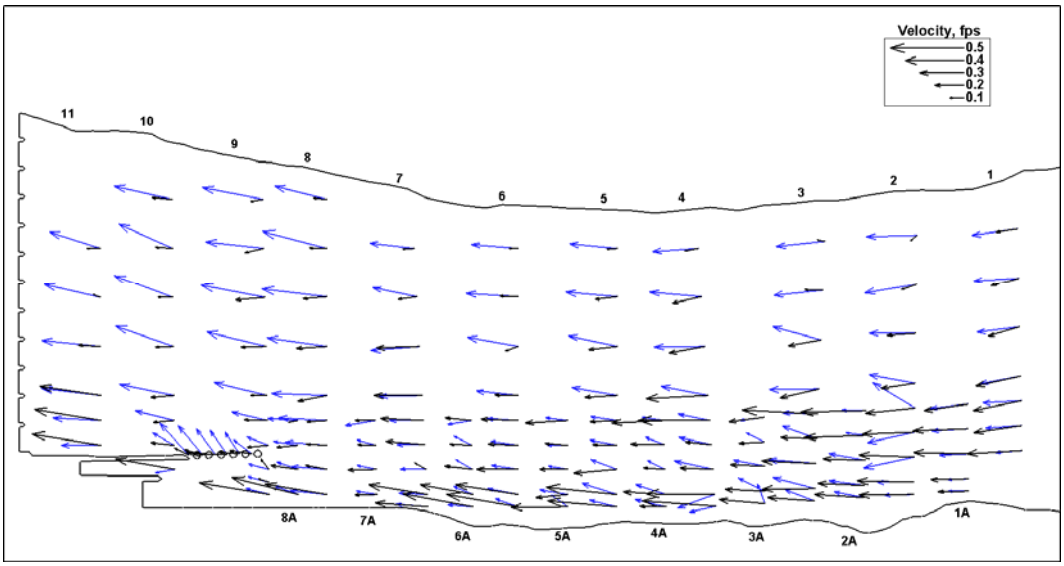

Figure 38. Plan B lock approach, extended weir material, *n* = 0.010, physical model data (blue), and numerical model results, *k* = 0.7, *n* = 0. 010 (black).

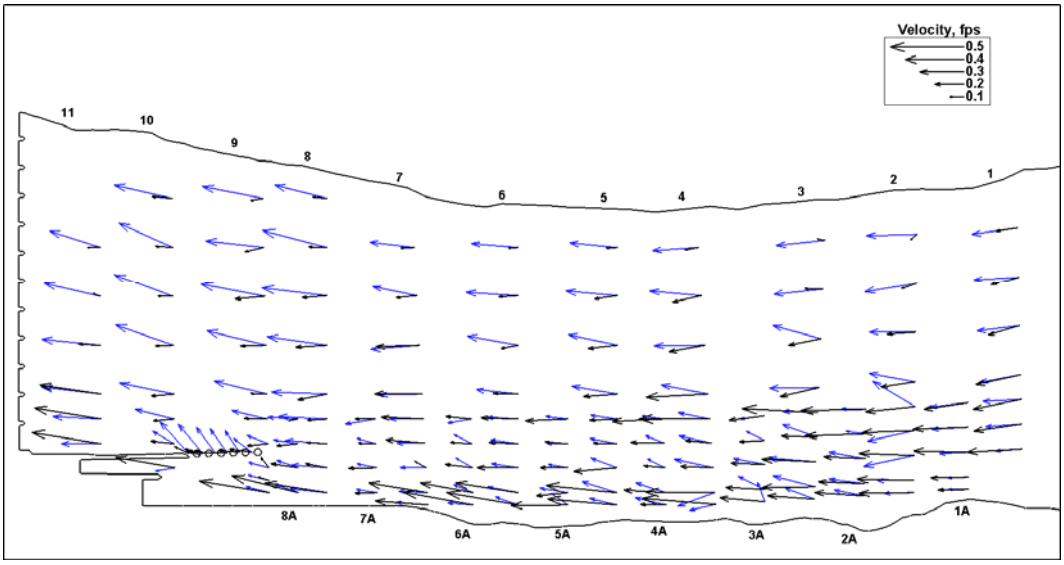

Figure 39. Plan B lock approach, extended weir material, n = 0.014, physical model data (blue), and numerical model results, k = 0.7, n = 0. 014 (black).

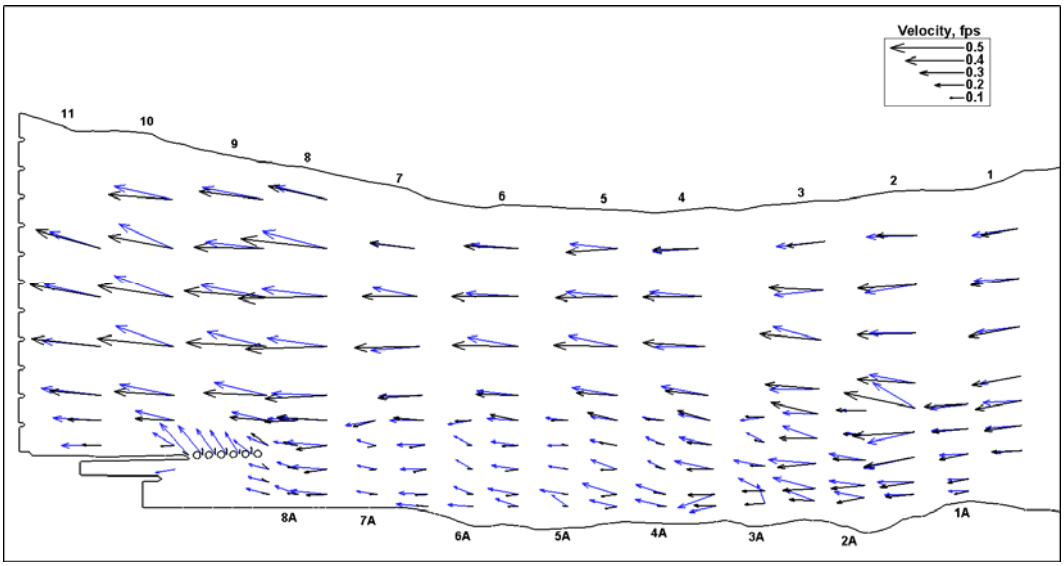

Figure 40. Plan B lock approach, extended weir material, n = 0.024, physical model data (blue), and numerical model results, k = 0.7, n = 0. 024 (black).

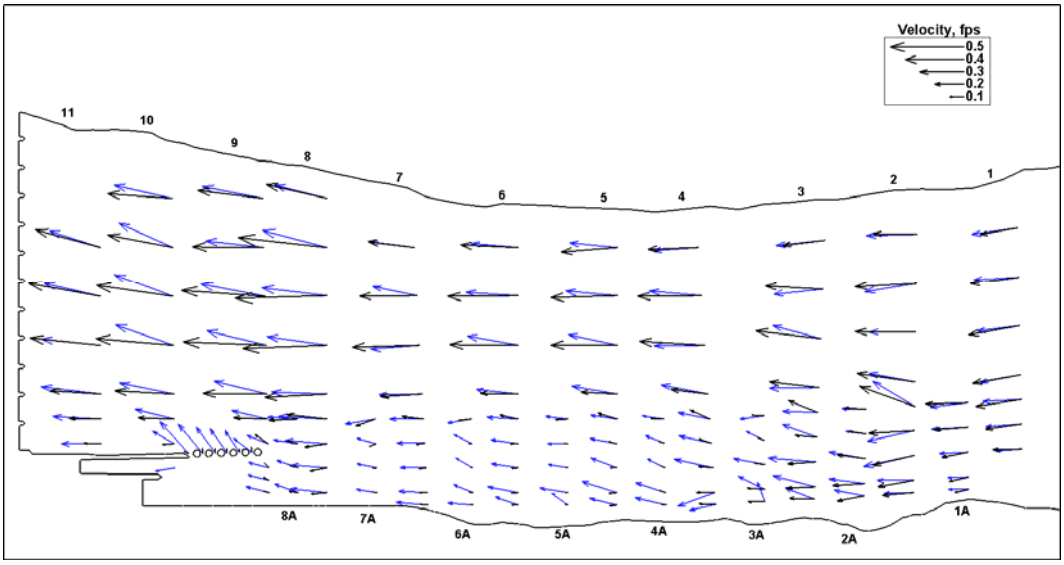

4 Summary

Experiments were conducted to assess the ability of the 2D depth-averaged numerical flow solver AdH to compute flow conditions in the approach to navigation locks. The velocity distribution computed with the numerical model was compared with similar data obtained on a physical model. The simulation results of two bathymetric configurations were evaluated. The Plan A lock approach had a rather simple bed geometry with a fairly flat bottom and simple side slopes. The Plan B lock approach had a series of submerged weirs upstream of the guard wall, placed normal to the navigation sailing line.

The numerical model accurately reproduced the flow distribution in the Plan A lock approach. The computed velocity magnitudes and directions compared well with those observed in the physical model (Figure 18). Evaluation of parameters found that the numerical model results best reproduced the observed physical model velocities when a scaling coefficient k of 0.7 and a Manning's n of 0.013 were used.

Other than the flow between the guard wall cells, the 2D model did well reproducing the velocity with the Plan A lock approach. However, the numerical model did not accurately reproduce the velocity with the Plan B lock approach. The flow between the guard wall cells and the flow over the weir field are two distinct features that made accurate computation of the velocity difficult. The numerical model equations assume that the bed slope is mild and that the pressure distribution is hydrostatic. The hydrostatic pressure assumption is not applicable to the accelerating flow between the guard wall cells and to the flow over a weir. The flow over weirs also violates the mild-slope assumption used in the equation development. The model over-predicts flow depth (and under-predicts velocity magnitude) when an adverse steep bed slope is encountered. Favorable steep bed slopes result in computed depths that are too shallow and velocities that are too large. These effects are attributed to both the mild-slope and hydrostatic pressure assumptions.

Experiments were conducted to determine if reasonable changes to model parameters could result in more accurate numerical model results. The Manning's n value for the weirs was varied from 0.008 to 0.024 while the

remainder of the flow domain used a Manning's n of 0.013. Furthermore, the area of Manning's n value coverage was increased by a weir width. Physical model data for Plan B show that as flow over the weirs approaches the lock entrance, it exits through the piers at a significantly greater velocity than calculated by AdH (Figure 32). The dissimilarity in velocity directions for Plan B indicates that 2D AdH is incapable of modeling sudden vertical contractions. This difference is attributed to the use of the hydrostatic pressure assumption, where the model does not carry vertical inertia as the flow contracts over the weirs.

Extending the weir material had an effect; however, it was not sufficient to reproduce the observed data. Smaller Manning's n values for the weirs resulted in more flow over the weir field, while larger weir n values reduced the flow over the weirs. The accuracy of the velocity of the flow between the guard wall cells did not improve in either case.

Additional numerical and laboratory experiments dealing with weir fields in lock approaches will have to be conducted if the accuracy of the computed velocity is to be improved. The numerical experiments would be directed toward developing a strategy for selecting model parameters to better represent the effects of submerged weirs. The laboratory effort would collect velocity distributions over the flow depth in areas such as the weir field. In and around areas where the flow is rapidly changing, the depth-averaged velocity can be accurately determined only when the velocity profile is known.

REPORT DOCUMENTATION PAGE

Form Approved
OMB No. 0704-0188

1. REPORT DATE *(DD-MM-YYYY)*	2. REPORT TYPE	3. DATES COVERED *(From - To)*
August 2013	Final report	

4. TITLE AND SUBTITLE

Validation of Modeling Flow Approaching Navigation Locks

5a. CONTRACT NUMBER

5b. GRANT NUMBER

5c. PROGRAM ELEMENT NUMBER

6. AUTHOR(S)

Carlos B. Bislip-Morales and Richard L. Stockstill

5d. PROJECT NUMBER

5e. TASK NUMBER

5f. WORK UNIT NUMBER

7. PERFORMING ORGANIZATION NAME(S) AND ADDRESS(ES)

Coastal and Hydraulics Laboratory
US Army Engineer Research and Development Center
3909 Halls Ferry Road
Vicksburg, MS 39180-6199;

8. PERFORMING ORGANIZATION REPORT NUMBER

ERDC/CHL TR-13-9

9. SPONSORING / MONITORING AGENCY NAME(S) AND ADDRESS(ES)

US Army Corps of Engineers
441 G. Street, NW
Washington, DC 20314-1000

10. SPONSOR/MONITOR'S ACRONYM(S)

11. SPONSOR/MONITOR'S REPORT NUMBER(S)

12. DISTRIBUTION / AVAILABILITY STATEMENT

Approved for public release; distribution is unlimited.

13. SUPPLEMENTARY NOTES

14. ABSTRACT

Experiments were conducted to assess the ability of the 2D depth-averaged numerical flow solver AdH to compute flow conditions in the approach to navigation locks. The velocity distribution computed with the numerical model was compared with similar data obtained on a physical model. The simulation results of two bathymetric configurations were evaluated. The Plan A lock approach had a rather simple bed geometry with a fairly flat bottom and simple side slopes. The Plan B lock approach had a series of submerged weirs upstream of the guard wall, placed normal to the navigation sailing line. Other than the flow between the guard wall cells, the numerical model accurately reproduced the flow distribution, velocity magnitudes, and directions compared in the Plan A lock approach; however, the numerical model did not accurately reproduce the velocity with the Plan B lock approach. Experiments were conducted to determine if reasonable changes to model parameters could result in more accurate numerical model results. Extending the weir material had an effect; however, it was not sufficient to reproduce the observed data. The accuracy of the velocity of the flow between the guard wall cells did not improve in either case. These effects are attributed to both the mild-slope and hydrostatic pressure assumptions.

15. SUBJECT TERMS

Navigation Lock
Validation
Computational
Hydrodynamic
AdH
Weir
Submerged
Depth-averaged

16. SECURITY CLASSIFICATION OF:			17. LIMITATION OF ABSTRACT	18. NUMBER OF PAGES	19a. NAME OF RESPONSIBLE PERSON Alejandro Sanchez
a. REPORT	b. ABSTRACT	c. THIS PAGE			19b. TELEPHONE NUMBER *(include area code)*
UNCLASSIFIED	UNCLASSIFIED	UNCLASSIFIED		42	